(2)

Technical Report 1412
March 1991

Cold Fusion Verification

M. H. North
G. F. Mastny
E. J. Wesley

NAVAL OCEAN SYSTEMS CENTER

San Diego, California 92152-5000

J. D. FONTANA, CAPT, USN
Commander

H. R. TALKINGTON, Acting
Technical Director

ADMINISTRATIVE INFORMATION

This work was performed by members of the Radiation Physics Branch, Code 524, Naval Ocean Systems Center, under the Office of Chief of Naval Research, Independent Research Programs.

Released by
E. J. Wesley, Head
Radiation Physics Branch

Under authority of
H. O. Porter, Head
Environmental Sciences
Division

ACKNOWLEDGEMENTS

The authors wish to thank the following persons for their helpful comments and support throughout this project: Al Gordon, Hugh Copeland, Al Zirino, and Aleta Wallace, Naval Ocean Systems Center; William Johnson and Howard Menlove, Los Alamos National Laboratory; Charles Scott, Oak Ridge National Laboratory; and John Moore, Scottsdale, AZ.

JG

SUMMARY

The objective of this work was to verify and reproduce experimental observations of Cold Nuclear Fusion (CNF), as originally reported in 1989 by Fleischmann, Pons, and Hawkins (see reference 1).

The method was to start with the original report and add such additional information as became available to build a set of operational electrolytic CNF cells. Verification was to be achieved by first observing cells for neutron production, and for those cells that demonstrated a nuclear effect, careful calorimetric measurements were planned.

The authors concluded, after laboratory experience, reading published work, talking with others in the field, and attending conferences, that CNF probably is chimera and will go the way of N-rays and polywater.

CONTENTS

FIGURES

TABLE

INTRODUCTION

The objective of this work was to verify and reproduce experimental observations of Cold Nuclear Fusion (CNF) as originally reported by Fleischmann, Pons, and Hawkins (reference 1). The method was to start with the original report and add such additional information as became available to build a set of operational electrolytic CNF cells. At the start of this work, it was expected that additional details on the proper construction of reliable cells would be available by the time the necessary materials and monitoring equipment could be gathered and set up. (Pons had announced that a paper containing just such information was to be published in the Fall 1989.)*

Verification was to be achieved by first observing cells for neutron production, and for those cells that demonstrated a nuclear effect, careful calorimetric measurements were planned. The reason for looking for neutrons first is this would be the most sensitive and immediate test of the presence of any putative nuclear effect rather than looking first for heat, which would require more extensive data analysis to confirm. The detection of neutrons is uniquely valuable as confirmation of the proposed fusion scenario as they are a product of the claimed and most likely reactions (1 and 2, table 1). They are also a product of most other conceivable reactions given the constituents of the cell. The exceptions are reactions 7, 8, and 11. Because of reaction 11, some of the cells were monitored with gamma ray detection equipment. Also, because of reactions 7, 8, and 11, it was decided to have the palladium anodes analyzed for ^{3}He and ^{4}He "ash," which would be expected to remain in the metal lattice once produced there.

Table 1. Some fusion reactions. The * indicates reactions involving significant constituents of a CNF cell.

Reaction Number	Reaction	Fusion Cross Section, Barns
* 1+	$D_1^2 + D_1^2 \rightarrow He_2^3(0.82MeV) + n(2.45MeV)$	10^{-2}
* 2+	$D_1^2 + D_1^2 \rightarrow T_1^3(1.01MeV) + H_1^1(3.02MeV)$	10^{-2}
* 3	$D_1^2 + T_1^3 \rightarrow He_2^4(3.5MeV) + n(14.10MeV)$	2
4	$D_1^2 + He_2^3 \rightarrow He_2^4(3.6MeV) + H_1^1(14.7MeV)$	2×10^{-3}
5	$T_1^3 + T_1^3 \rightarrow He_2^4(3.8MeV) + 2n(7.6MeV)$	10^{-2}
6	$He_2^3 + He_2^3 \rightarrow He_2^4(4.3MeV) + 2H_1^1(8.5MeV)$	
* 7#	$D_1^2 + Li_3^6 \rightarrow 2He_2^4 + 22.4MeV$	
* 8#	$H_1^1 + Li_3^7 \rightarrow 2He_2^4 + 17.4MeV$	10^{-3}
9	$Li_3^6 + n \rightarrow He_2^4 + T_1^3 + 4.6MeV$	10^{-3}
* 10#	$Li_2^7 + D_1^2 \rightarrow Be_4^8 + n + 15.0MeV$	10^{-6}
* 11	$H_1^1 + D_1^2 \rightarrow {}^3_2He + \gamma(5.4MeV)$	

+ Branching ratio 1:1

Natural lithium contains 7% ^{6}Li and 93% ^{7}Li.

*Reported in alt.fusion (Usenet) 1989.

In the meantime, it was reported in various places (references 2 and 3)* that neutrons had been observed in certain circumstances in conjunction with D_2 gas loading of titanium and other metals and materials. While waiting for further developments on the electrolytic cell front, we pursued the phenomenon of fractofusion, as the gas experiments were called. We will describe the results of both of these efforts in this report.

NEUTRON DETECTOR

The neutron detector used for these tests was a completely packaged unit built into a metal suitcase that afforded electrostatic shielding for the detectors and self-contained electronics. It was battery-powered, although it was on charge for most of the long tests. The sensor element consists of 34 ^{3}He detectors arranged in three independent layers in a solid moderating block (see appendix A). The count from each of the three layers as well as the sum of all the detectors were brought out and recorded separately. The neutron measurements were made with both the neutron detector and the sample tested in a cave made of thick moderating material that surrounded the two units on the sides and bottom. The detector itself was sealed inside a plastic bag with desiccants to minimize the effects of condensation from the liquid nitrogen (LN_2) used to temperature cycle the Ti + D_2 samples.

The overall detection efficiency for the suitcase detector in the cave using ^{252}Cf sources was 10.3%. That is, 10.3% of all the neutrons emitted by the source were captured and counted by the detector. The calibration measurements were made with the high-pressure gas cylinder used for the Ti + D_2 tests in place, and it was assumed that the changes in efficiency when the dewar with LN_2 was in place around the pressure vessel or the electrolytic cell was in the test position were minor and did not materially change detection capability.

The data were recorded on two systems. The three individual layer data were directed to three 4096-multichannel scaler inputs controlled by a 80386 microprocessor. A continuous record of rate versus time was recorded for each input. The time interval per channel (normally 5 or 50 milliseconds in these tests) and the total number of 4096 records dumped to a 40-megabyte disk were selectable at the keyboard. The data were processed after the tests for changes in total count from all three layers and for the number of time intervals with multiple neutrons in individual layers or in any combination. The multiple neutrons could be attributed to bursts of neutrons, a characteristic prominent in cold-fusion literature. The three-layer data also afforded a reliability check for electrical interference or detector malfunction.

With the second recording system, the integrated count from the sensor was treated either of two ways: (1) the total count was recorded on a 1024-multichannel analyzer and displayed for realtime monitoring normally in 1- or 10-second intervals, or (2) the signal was directed to a coincidence circuit to test for multiple neutrons and that result taken to the multichannel analyzer. The coincidence window was normally set to 250 microseconds. The moderating time of the cave-detector setup was measured at 56 microseconds using a low level ^{252}Cf source, which produces approximately 3 neutrons per fission. Based on these data, the 250-microsecond window was almost 4.5 times the moderation time constant and should include 99% of the neutrons issued in multiples from a single reaction. The number of coincidence events were summed at the multichannel analyzer in 10-, 40-, or 80-second intervals, depending upon the expected length of the test.

*Also reported in sci.physics.fusion (Usenet) 1989.

NEUTRON BACKGROUND

The background counting rate from cosmic ray neutrons averaged approximately 1 count/second (cps). Over the months of the measurement, the background taken before and/or after each run varied from 0.88 to 1.1 cps. The changes reflect the presence of different test cell configurations within the measurement cave as well as small changes in cosmic neutron background observed over multiday periods. The one sigma error bar on these measurements was normally less than 0.005 cps.

The counting rate from background from the 250-microsecond coincidence circuit with the pressure vessel in place averaged 0.0095 cps. These counts are attributed to cosmic rays that react and produce bursts of neutrons from materials within the cavity. As a test, the pressure vessel was removed and 71 kg of Pb in the form of bricks were placed in the cavity with the detector. The cosmic ray interaction rate increased significantly and the coincidence rate jumped to 0.204 cps.

FRACTOFUSION DISCUSSION

A mechanism has been proposed by Takeda and Takizuka (reference 4) and others (reference 5) to account for some of the more modest observations of CNF. This has been dubbed fractofusion and is based on earlier work on fractoemission (references 6, 7, and 8). The phenomenon occurs when microcracks form in materials and charges appear on the crack surfaces due to uneven breaking of bonds. Very large electric fields may result that may persist long enough to accelerate ions and other free particles in the crack to high energy. If the ions happen to be deuterium, they may acquire sufficient energy (up to 100 kev) to undergo fusion. This is actually "hot" fusion. Figure 1 illustrates the situation in which a crack of length l, width w, and depth d forms in palladium. The crack may be caused by physical stress, deuterium loading, or other mechanical means. In the case of a metal such as palladium, the charges formed will quickly neutralize due to currents around the crack (arrow). The question becomes one of comparing the RC time constant for this process to the time it takes for an ion to accelerate to say 10 kev before the fields dissipate. It must also be true that the crack forms in a time less than RC. Based on some fairly reasonable assumptions, we can calculate these times. The following discussion is based on a talk given by F.J. Mayer, University of Michigan at the Workshop on Cold Fusion Phenomenon, Sante Fe, NM, May 23-25, 1989.

First, we show the limits placed on RC by the speed of crack formation. From figure 2 we see that if

$$\mathrm{RC} > \frac{w}{v_s} \tag{1}$$

where

$$v_s \text{ (speed of sound)} \approx 2000 \text{ m/s} \tag{2}$$

the charges will not have sufficient time to move during crack formation. Thus, for two reasonable values of w it must be that

$$w = 0.1 \text{ micron} \rightarrow \text{RC} > 50 \text{ ps} \tag{3}$$

$$w = 1.0 \text{ micron} \rightarrow \text{RC} > 500 \text{ ps} . \tag{4}$$

Next we calculate RC. The resistance of a conductor is given by

$$R = \frac{\varrho(2d)}{A'} = \frac{2\varrho d}{1\delta} \tag{5}$$

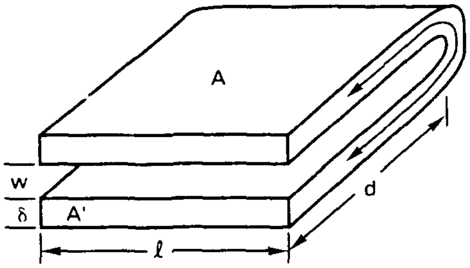

SPONTANEOUS CRACK
IN PALLADIUM

$R = \frac{(2d)}{A'} = \frac{2\rho d}{\rho s}$

ρ(resistivity of Pd) = 11×10^{-8} ohm-m

d ~ 1000 microns

δ ~ 100 Å

$C = \epsilon_0 \frac{A}{w} = \epsilon_0 \frac{\ell d}{w}$

$\epsilon_0 = 8.85 \times 10^{-12}$ farad/m

$RC = 2\epsilon_0 \frac{\rho d^2}{w\delta} = \frac{2 \times 10^{-16}}{w}$ s

Figure 1. Electric fields produced in the crack will decay with time constant RC as the surface change density shorts out around the crack.

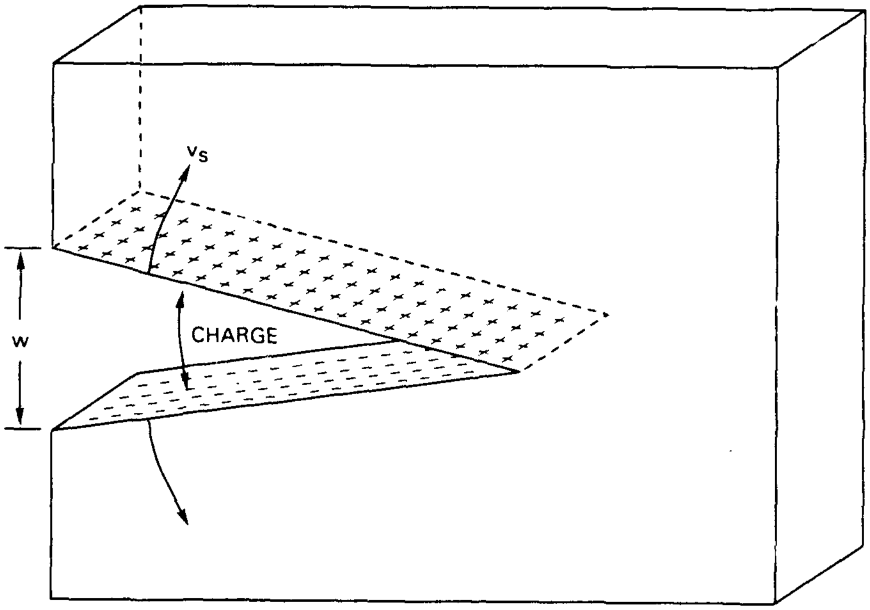

Figure 2. Crack of width w forms in bulk material at speed of sound, v_s.

where (refer to figure 1)

$$\varrho \text{ (resistivity of Pd)} = 11 \times 10^{-8} \text{ ohm-m} \tag{6}$$

$$A' \text{ (area normal to current flow)} = \ell\delta \tag{7}$$

$$\delta \approx 100 \text{ Å} = 1 \times 10^{-8} \text{ m} \tag{8}$$

while the capacitance of a parallel plate capacitor is

$$C = \epsilon_o \frac{A}{w} = \epsilon_o \frac{\mathrm{ld}}{w} \tag{9}$$

where

$$\epsilon_o \text{ (permittivity)} = 8.85 \times 10^{-12} \text{farad/m} \tag{10}$$

$$A \text{(area of capacitor)} = \mathrm{ld} \; . \tag{11}$$

Therefore, we have

$$\mathrm{RC} = 2\epsilon_o \frac{\varrho \mathrm{d}^2}{\mathrm{w}\delta} \tag{12}$$

$$\cong \frac{2 \times 10^{-10} \mathrm{d}^2}{w} s. \tag{13}$$

Referring to figure 3 we see that for

$$w = 0.1 \text{ micron} \rightarrow d > 200 \text{ microns} \tag{14}$$

$$w = 1.0 \text{ micron} \rightarrow d > 2000 \text{ microns} \tag{15}$$

that is, d must be greater than these values in order that RC will be long enough. The time for a deuterium ion to accelerate across the width of the crack may be determined by integrating the force equation for a charge in a uniform electric field

$$F = eE = m\frac{d^2x}{dt^2} \tag{16}$$

where

$$e \text{(charge of ion)} = 1.6 \times 10^{-19} C \tag{17}$$

$$E \text{(electric field)} = \frac{\sigma}{\epsilon_o} \tag{18}$$

$$\sigma \text{ (surface charge density of capacitor)} \tag{19}$$

$$m \text{ (mass of ion)} = 2 \times 1.67 \times 10^{-27} \text{kg} \tag{20}$$

so upon integrating over x from 0 to w we have

$$t = \sqrt{\frac{2mw}{eE}} \; . \tag{21}$$

For the surface charge density, we assume one charge per 10 square lattice sites, which for palladium (lattice constant 4 Angstroms) amounts to

$$\sigma = \frac{1.6 \times 10^{-19} C}{10(4 \times 10^{-10})^2 m^2} \cong 0.1\ C/m^2\ . \tag{22}$$

This gives an electric field in the crack of

$$E \cong 1 \times 10^{10} \text{ volts/m} \tag{23}$$

so that

$$t \cong 2 \times 10^{-9} \sqrt{w}\ s\ . \tag{24}$$

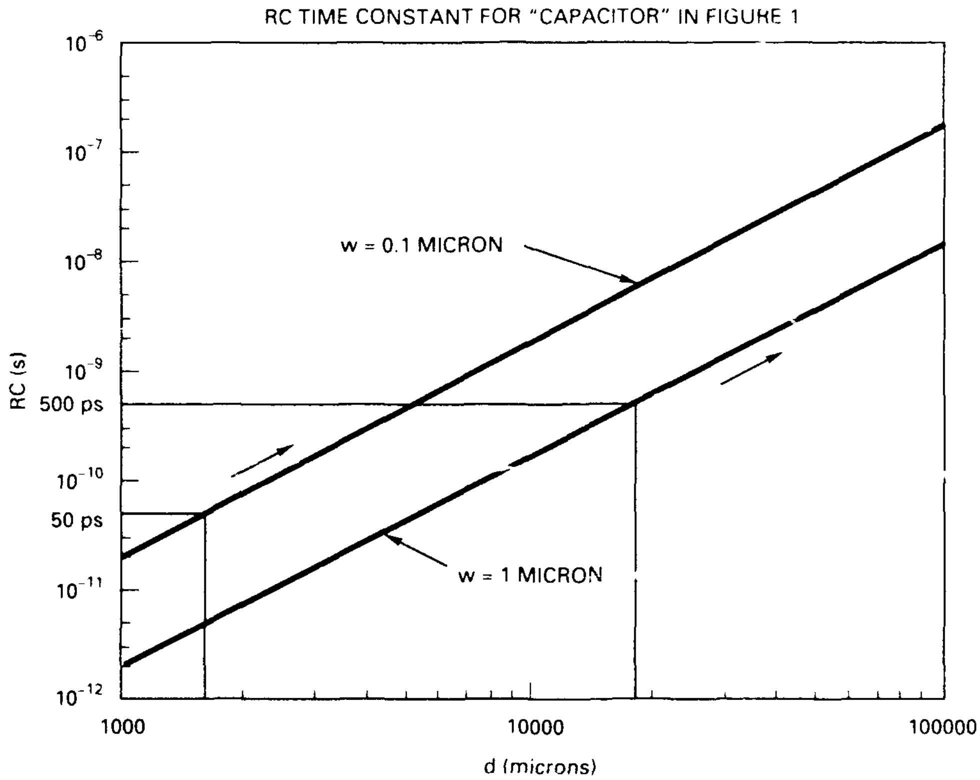

Figure 3. Discharge time for free charges around a crack of width w and depth d.

Comparing this t with RC we see for our two cases

$$w = 0.1 \text{ micron} \rightarrow t > 0.6 \text{ ps and RC} = 80 \text{ ps} \tag{25}$$

$$w = 1.0 \text{ micron} \rightarrow t > 2 \text{ ps and RC} = 800 \text{ ps} \tag{26}$$

so that there is plenty of time for the acceleration of the ions. Also note that the ion will acquire an energy (in ev) of

$$E = \acute{E}w \tag{27}$$

in traversing the crack. Having demonstrated the plausibility of having 10 kev D ions in palladium, the next issue is a cross section for fusion and fusion rates.

Clearly, what is important here is the number of fusions per crack rather than the number of fusions per D per second, as is usually reported. The reason is that for the mechanism of fractofusion these fusions are not continuously produced and, therefore, the relevant rate becomes the crack rate. The fusions per crack are

$$\frac{\#}{\text{crack}} = \left[\frac{\sigma}{a^2}\right]\left[\frac{\eta S}{a^2}\right] \tag{28}$$

where the first factor in square brackets is the fusion probability for 1:1 Pd-D and the second factor in square brackets is the number of ions in the crack. Here

$$\sigma = \sigma(\text{E}) \text{ (fusion cross section)} \tag{29}$$

$$a \text{ (lattice constant for Pd or Ti)} \approx 4 \text{ Å} \tag{30}$$

$$\eta \text{ (fraction of unbalanced charge)} = 0.1 \tag{31}$$

$$S \text{ (area of crack)} \approx 1000\,\mu \times 100\,\mu = 1 \times 10^{-7}\text{m}^2\,. \tag{32}$$

The cross section is a function of energy and is shown in figure 4. This curve is from an empirical formula given by Artsimovich (reference 9). Note that this is the cross section for monoergic deuterons and not for a plasma. Scaling this curve by the above factors gives figure 5, the number of

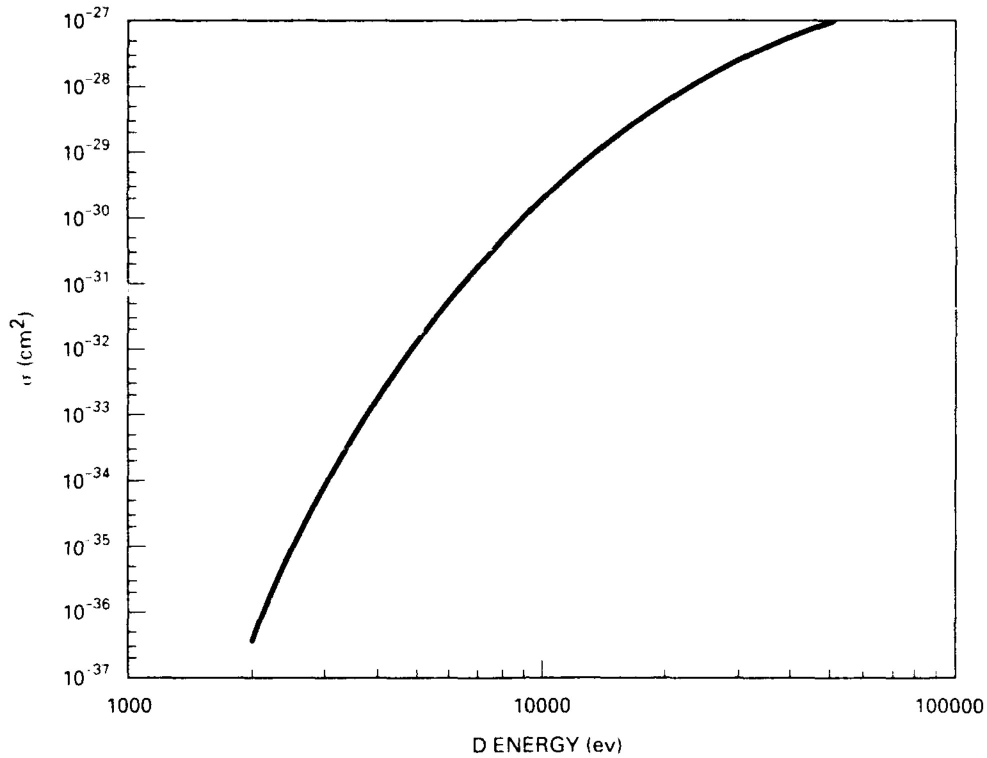

Figure 4. Fusion cross section (monoergic deuterons).

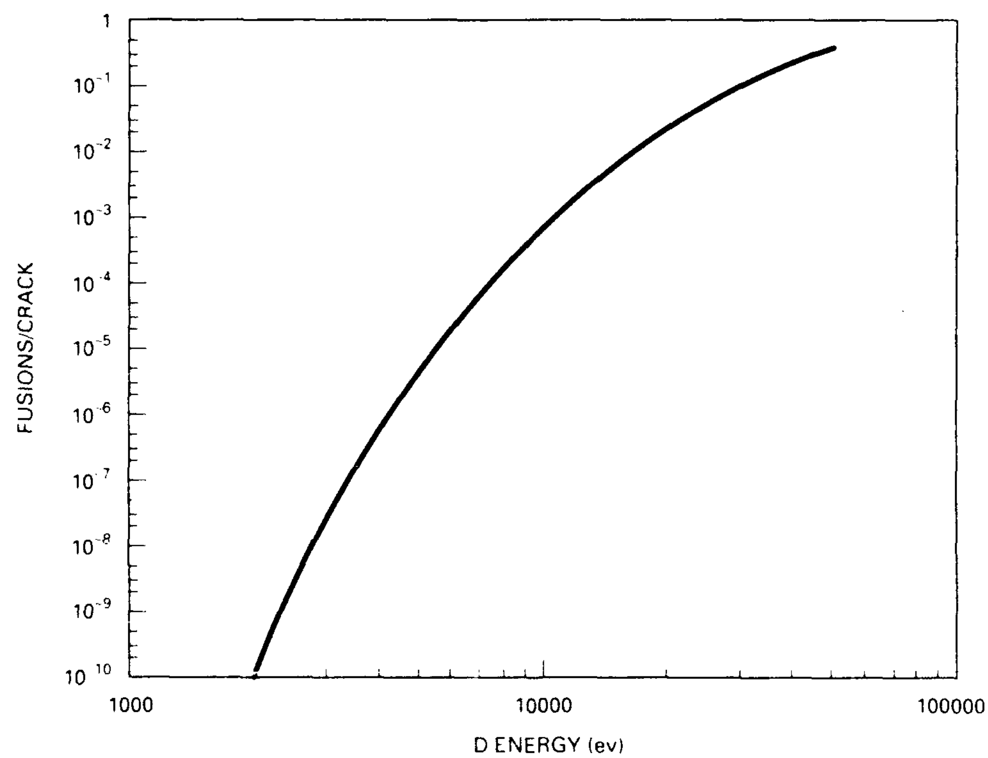

Figure 5. Fusions per crack (crack area 10^{-7} m^2).

fusions expected per crack as a function of D energy. Note that for energies of a few 10s of kev, the number of cracks required to produce a neutron gets down to about 10 or so. Thus, it seems plausible that under some set of favorable circumstances fusions might be detectable from this mechanism.

FRACTOFUSION EXPERIMENTS (Ti + D_2 GAS TESTS)

The principal goal in the Ti + high pressure D_2 gas tests was to identify neutrons generated as the deuterium-loaded titanium was temperature-cycled from room temperature to 77°K (with LN_2) and back to room temperature. It has been suggested (reference 4) that the neutron could be the result of deuterium atoms accelerated by voltages generated when the loaded titanium lattice cracks under stresses generated by the changing temperature. Deuterium atoms accelerating in the gap, collide and react with other deuterium atoms in the gap or bound in the titanium. Early reports of neutron bursts (reference 10) using this approach were later withdrawn, but the mechanism of accelerating particles by fracturing materials, particularly insulators, is well established (reference 11) and the possibility of generating neutrons by fractofusion is worth investigating.

The general test setup was described earlier. The pressure vessel was a 1-liter, stainless-steel bottle loaded with 225 grams of "pure" titanium in the form of strips 1 cm wide, 18 cm long, and 0.025 cm thick and pressurized to 600 psi (room temperature) with deuterium gas (99.8 atom % D). The titanium was cut from sheets, degreased, and then dried in a vacuum oven at 496°C for at least 96 hours. Midway through the tests, the titanium strips were removed, examined, and then degreased and dried a second time before reloading and pressurizing the pressure vessel. A thermocouple was attached to the outside of the pressure bottle, and the voltage was referenced to an ice bath. The output was recorded every 10 seconds throughout each temperature cycle.

All told, six complete temperature cycles were recorded and analyzed for neutron production. Five were high-pressure runs from room temperature to liquid nitrogen and back to room temperature. One started at high pressure was cooled to liquid nitrogen temperature and held for approximately 1 hour while the D_2 gas was released and the pressure vessel evacuated to 2×10^{-5} torr. The unit was then warmed slowly to room temperature. The temperature cycle data cover approximately 124 hours. In addition, aperiodic background runs were made at room temperature with the pressure vessel in place 30 hours.

The limits of detection for the overall system are determined by the detection efficiency (i.e., 10.3% per emitted neutron), the background rates for each mode, and the integrating time used for the measurement. For the gross count, with a background rate of 1 cps and a 1-second measurement interval, an extra 6 or 7 cps for several seconds would be statistically significant. The probability of 8 counts (7+1 from background) from background only is approximately 10^{-6}, but there were 0.5×10^6 sample periods in the 124 hours of testing and one or even two bins with 8 counts in the overall period are to be expected. To consistently add 6 or 7 extra counts to a 1-second time bin, the neutron rate in the pressure vessel should be 60 to 70 n/s. If the time interval is 10 seconds, the neutron rate could be 17 to 18 n/s, and if you integrate for 1 minute a rate of 6 n/s for several minutes would be readily detected and recognized. In the coincidence mode (250 microsecond), the summing interval was 40 seconds or more. The average count per 40 seconds for background of 2s or more was approximately 0.4. An increase of 5 or more counts in several time bins would be significant. While only two neutrons are needed for a coincident event, to consistently detect bursts at the level indicated for the gross-count measurement, the event should produce 10s to 100s of neutrons (because of the efficiency factor) and the overall production rate comparable to the gross count test

(because of the efficiency factor) and the overall production rate comparable to the gross count test with a 1-minute integration period. That is, the bursts must come often enough to maintain a gross-count rate as indicated above.

There were no significant differences in total or coincident neutron count rates between the known background data and the data recorded during the temperature cycles. With one exception, the count rate distributions for both types of measurements followed poisson statistics. The exception, 50 sets of 2 or more neutrons/50 milliseconds in a period of 204.8 seconds, 4096 bins, when the average number for that period was 6, cannot be explained as a statistical oddity. The total number of neutrons in the 204.8 seconds was slightly less than the average for that period calculated for all the measurements. Most of the multiple events were distributed randomly over the whole 204.8-second measurement, and the 204.8-second data sets just before and just after the anomaly were close to the mean in terms of total count and multiple neutrons per time bin. Because the total count in the data set did not increase and the excess multiple count appeared spread throughout the one data set but not in the data sets before or after, it appears the excess is a recording glitch rather than a string of multiple neutron events in the pressure vessel.

The only conclusion that can be drawn from the measurements is there were no neutron events above background and, hence, if there is an effect it is too small to be observed with the present monitoring scheme.

CALORIMETRY

One consensus reached at the Cold Fusion Workshop (Sante Fe, May 1989) was that to properly measure the total energy flux in a CNF cell some sort of closed cell calorimetry would be required. The original claims of enormous excess heat production of these type of cells were based on open cell calorimetry, in which elaborate calculations and assumptions were required to determine quantitative heat fluxes (reference 12). Moreover, an open cell requires constant replenishment of the electrolyte as the experiment progresses, allowing the possibility of contamination of the system and complicating the calorimetry.

In the closed system, on the other hand, the cell is sealed immediately after the expulsion of excess oxygen (used to determine the degree of D loading of the palladium electrode) and remains sealed through the rest of the experiment. In the cell is a catalyst that recombines the liberated deuterium and oxygen as it is produced, this greatly simplifies the subsequent energy analysis. The entire cell is submerged in a constant temperature water bath. The water bath temperature is maintained at an elevated temperature relative to the room temperature by an immersion heater the power to which is continuously monitored. Power to the cell also is continuously monitored, and any change in heat output from the cell is determined by observing fluctuations in heater power required to maintain constant temperature. This continuous record of power in the system is integrated at the conclusion of the experiment to determine total energy supplied to and received from the cell. This technique requires far fewer assumptions to calibrate and maintain than the open cell method.

We have built such a closed cell system for the determination of total energy output of our cells. Figure 6 shows the setup for a single cell; however, the computer is capable of handling up to six cells simultaneously. The loop labeled Pt is meant to represent the catalyst for the recombination of deuterium and oxygen. Originally, it was to be made of platinum but was subsequently replaced with a

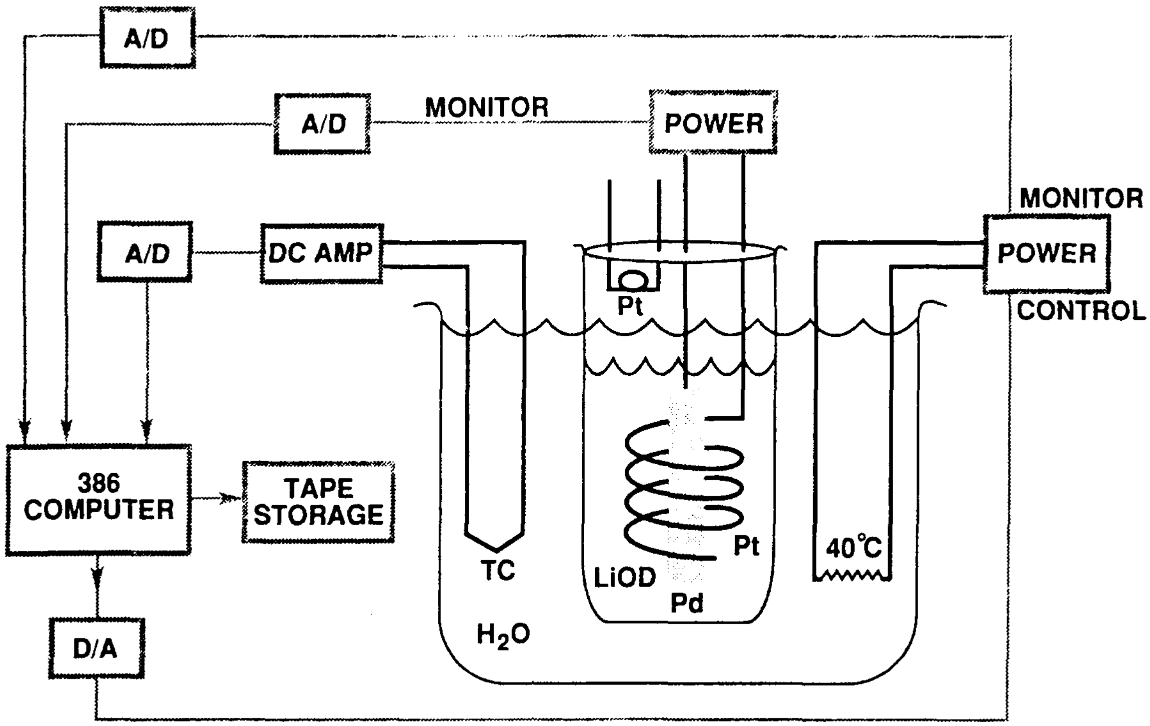

Figure 6. Pons-Fleischmann-Hawkins cell schematic.

device called a Catalator from Hydro-Cap Corporation. This particular catalyst is capable of recombining 3 amperes of hydrogen continuously. The water bath temperature is continuously monitored by the computer through the use of a thermocouple (TC). Observed temperature fluctuations are compensated for by the controllable power supply attached to the immersion heater. At the same time, power to the heater and power to the cell are collected by the computer and along with temperature are written to mass storage. To store the massive amounts of data to be collected, it was originally decided to use digital audio tape (DAT) technology and, in fact, the tape units were purchased; however, the required interface software was not written so resources could be shifted to the (by then) more promising fractofusion work. Nevertheless, there is a limited data storage capability on a hard disk that would be adequate for calibration and short runs. Should more information become available in the future on the construction of working CNF cells, this monitoring system is available and on the shelf.

ELECTROCHEMICAL CELLS

We have constructed three electrochemical cells from the description given by Pons, et al., (reference 1) and what additional information we have been able to obtain. The physical construction of the cells is described in appendix B. With two of these cells and two earlier cells, we have a combined observation time of over 500 hours without the detection of a single neutron that cannot be readily explained by the natural neutron background. With one of the earlier cells (without calorimetry), we observed a rise in heat output relative to a control cell (H_2O), however there was no

neutron signal. Along with this rise in heat output, we also noted a rise in cell resistance, and since the cell was being operated at constant current, the I^2R heating was probably responsible for the increased heat. After the completion of this particular run, we sent the electrodes to Sandia National Lab to be analyzed for ^3He and ^4He. The results were negative (reference 13). During this run we were also monitoring for gamma rays. None above background was seen. It was this experience that convinced us to redesign our cells around Teflon, since the consensus in the field was that the alkali electrolyte was leaching contaminants from the glassware causing unpredictable results.

Considerable effort went into the construction of these cells to assure a minimum of contamination, and the cells are unique in this field having been constructed of Teflon. Should, at some future date, additional information become available these cells will be on the shelf and ready for modification with minimum effort.

CONCLUSIONS

We believe, based on our own laboratory experience, reading published work, talking with others working in the field, and attending CNF conferences, that CNF is probably chimera and will go the way of N-rays and polywater. To date, no one, including Pons and Fleischmann, has been able to construct a so-called CNF electrochemical cell that will produce excess heat (presumably from fusion) and the necessary nuclear particles simultaneously and on demand. (Pons' promised paper, which was to give a detailed description on how to construct a working cell, never appeared). All of the positive results of which we are aware are very marginal (i.e., low signal-to-noise ratio) or suffer from misinterpretation or blunder. In one case even fraud has been suggested (reference 14).

On the other hand, in spite of our negative results with fractofusion, we believe this phenomenon may have practical application for the Navy as a controllable neutron source and that warrants further study. Fractoemission is a real, demonstrable effect, which can be explained entirely within the framework of known electromagnetic processes. Fractofusion is a plausible extension of this effect based on known nuclear processes. As such, we believe it to be a legitimate area of research and development.

REFERENCES

1. Fleischmann, M., S. Pons, and M. Hawkins. 1989. *J. Electroanal. Chem. 261*, 301 and errata in *J. Electroanal. Chem. 263*, 187.
2. Menlove, H. O. 1989. Workshop on Cold Fusion Phenomenon, Sante Fe, NM, May 23-25.
3. Science News *137* (2/10/90), 87.
4. Takeda, T., and T. Takizuka. 1989. *J. Phys. Soc. Japan 58*(9), 3073.
5. Science News *137* (2/10/90), 87.
6. Klyuev, V. A., Yu. P. Lipson, et al. 1986. *Sov. Tech. Phys. Lett. 12*(11), 551.
7. Deryagin, B. V., V. A. Klyuev, et al. 1986. *Kolloidnyi Zhurnal 48*(1).
8. Dickinson, J. T., E. E. Donaldson, and M. K. Park. 1981. *J. of Mater. Sci. 16*, 2897.

9. Artsimovich, L. A. 1964. *Controlled Thermonuclear Reactions*. Gordon and Breach.

10. De Ninno, A., et al. 1989. *Europhys. Lett. 93*, 221.

11. Dickinson, J. T., E. E. Donaldson, and D. B. Snyder. 1981. *J. Vac. Sci. Technol. 18*(2), 238.

12. Fleischmann, M., S. Pons, et al. 1990. *J. Electroanal. Chem. 287*, 293.

13. Oliver, B. M., and K. L. Wilson. 1989. "Helium Measurements in 'Cold Fusion' Palladium", see Appendix C.

14. Taubes, G. News and Comment, *Science*, 1299.

APPENDIX A

PORTABLE NEUTRON ARRAY

PORTABLE NEUTRON ARRAY

A compact, self-contained neutron instrument utilizing a sandwich detector array has been designed. The array design was optimized for detecting a "moderated" fission source over ground at a range of 100 ft. The array contains 34 ^{3}He tubes and consists of an outer, thermal-neutron detector comprising a bare layer of tubes completely surrounding the array, and an inner, fast-neutron detector comprising 10 tubes imbedded in a polyethylene moderator. The instrument will be housed in a light-weight aluminum briefcase and will be completely self-contained with rechargeable batteries and a cassette recorder for a permanent time-history recording of the neutron pulse-rate from the detector. The main power switches will be internal, and the operating controls will be accessible through a 1" X 3" port near the handle. A digital readout display will also be visible through this port. The functional aspects of the displays and controls were designed to meet two objectives: (1) to evaluate different readout and data analysis concepts, and (2) to provide a device which could be used on an interim basis in the field.

Following is a list of design specifications and a brief description of the operation of the instrument.

DESIGN SPECIFICATION:

Instrument Size and Weight: 5-3/4" wide X 13" high X 21" long and 35 lbs.

Detector Array: Size and Weight: 4-3/4" X 10-9/16" X 20" and 24 lbs. Tube Complement: 34 3-atm. pressure, 1" diam. ^{3}He proportional counters, 17-3/4" sensitive length. Sensitivity: 1 cps (net) for a $2X10^5$ n/sec "moderated" fission source 100 ft away and 7 ft above the ground; 2 cps background.

Controls: Internal: Power On; Detector On; Clock Reset. Operating: Display On; Record On; Count/Rate Mode Selector.

Displays: Four 3-digit, 7-segment LED display registers; one register for time and three for neutron data.

Recording: Incremental cassette recorder; 12-bit serial data word, 2-track complimentary NEZI format; 10 words/sec; ~4 hrs continuous recording per cassette.

Battery Complement and Life: 10 size "C" rechargeable NiCd batteries; nominal 12 hrs life with continuous readout display and recording.

OPERATION:

Internal Controls - The "Power" switch is the overall on-off control and by itself turns on a master clock which provides a time base for an entire operational event. This can be nearly 3 days long if the instrument usage during this period is less than the operational battery life. The "Detector" switch turns the remainder of the instrument on.

Operating Controls - The "Display" and "Record" switches enable these functions to be turned off when not needed to conserve battery power and recorder tape. The mode switch selects one of two operating modes of the instrument. In the "Count" mode, the instrument is a manually controlled 3-channel counter; the four registers display the number of pulses from the inner fast-neutron detector, the front-thermal and back-thermal detectors, and the counting time in seconds, respectively. In the "Rate) mode, all three neutron data registers indicate the gross counting rate from the detector, each register having a different time base. These are 1, 10, & 30 seconds. A buffer storage is used so that the display "holds" for the duration of the time base. The running time in seconds is displayed on the "Time" register which is reset every 480 seconds (8 min) and is

synchronized to the master clock and recorder. This allows correlation of events and recorded data to the nearest second.

Recorder - Recording is at a precise rate of 1 word every 0.1 sec. Each word consists of three 4-bit binary numbers which represent the number of counts from each section (front, back and inner) of the detector during the 0.1 sec period. The probability of overflow of the 4-bit number ($\gtrsim 15$ counts) is essentially zero at rates of 60 c/second and less than 0.1 at 100 c/sec per detector section. A file mark (blank word) followed by the running time in minutes is recorded every 8 minutes and whenever the recorder is turned on or off.

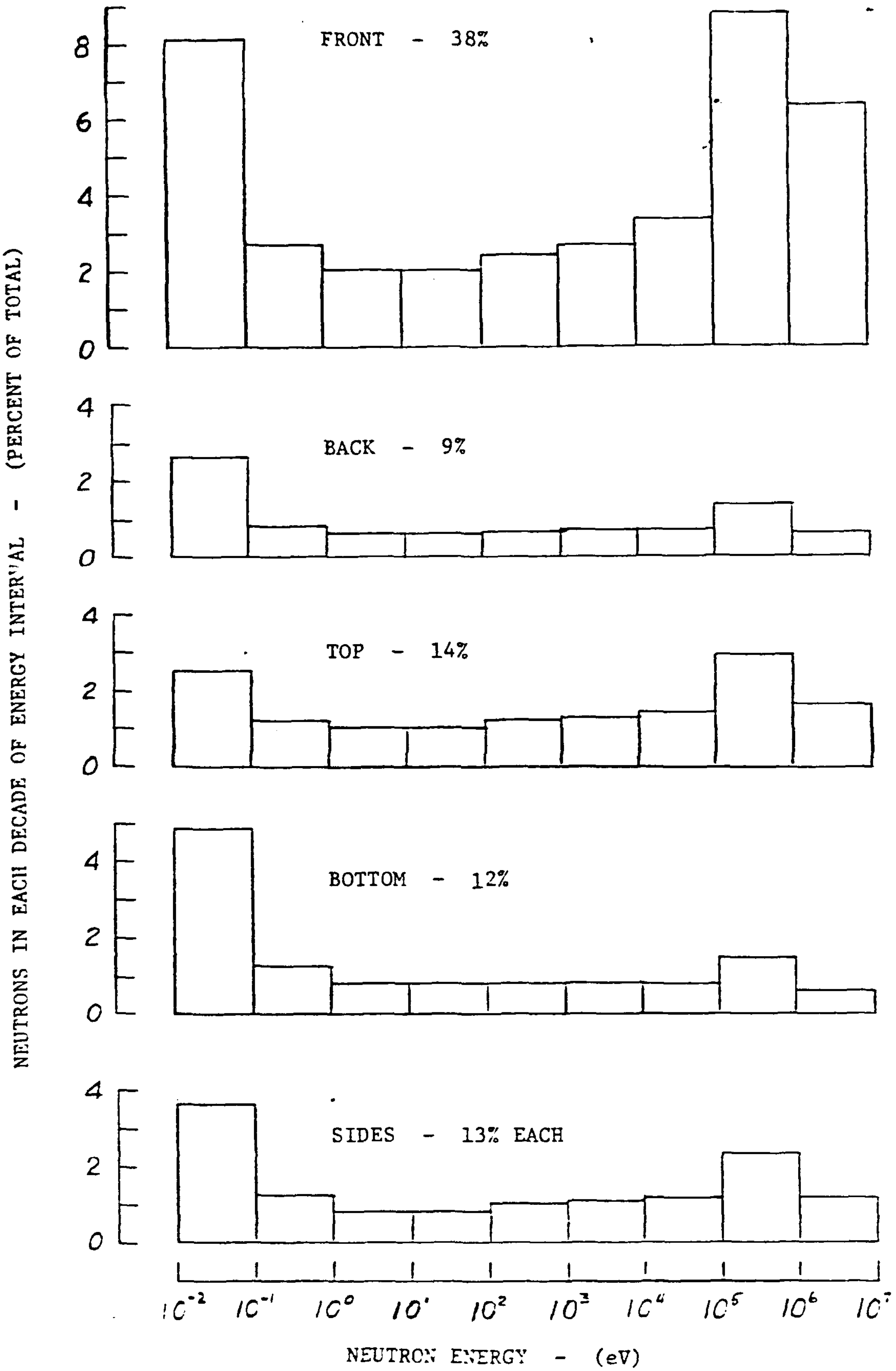

ENERGY AND DIRECTIONAL DISTRIBUTION OF NEUTRONS 7 FT. ABOVE THE GROUND AND 100 FT. FROM A MODERATED FISSION SPECTRUM SOURCE. SOURCE 7 FT. ABOVE THE GROUND.

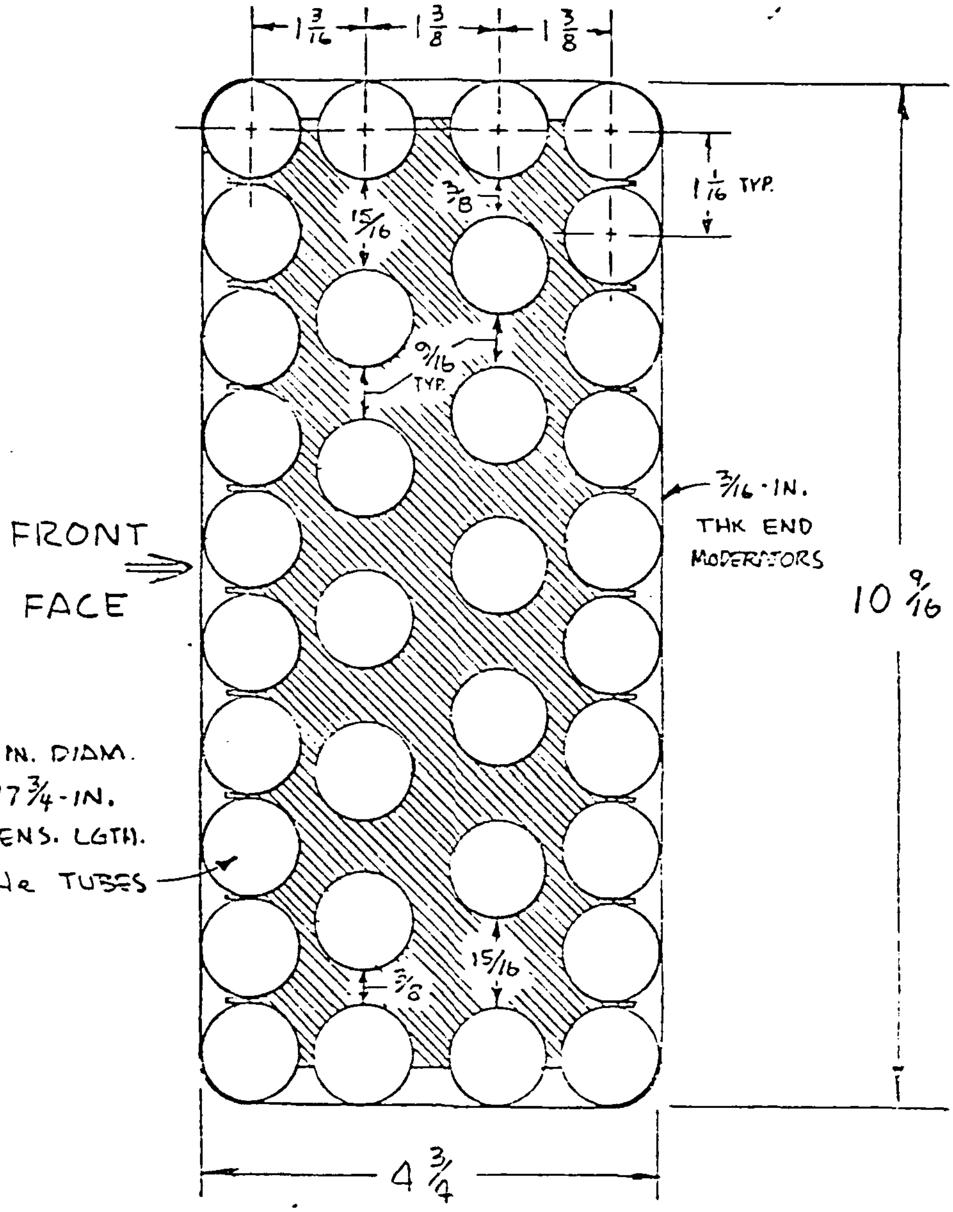

(U) FIG. 1 CROSS SECTION OF 34-TUBE ARRAY DETECTOR SHOWING TUBE-MODERATOR CONFIGURATION

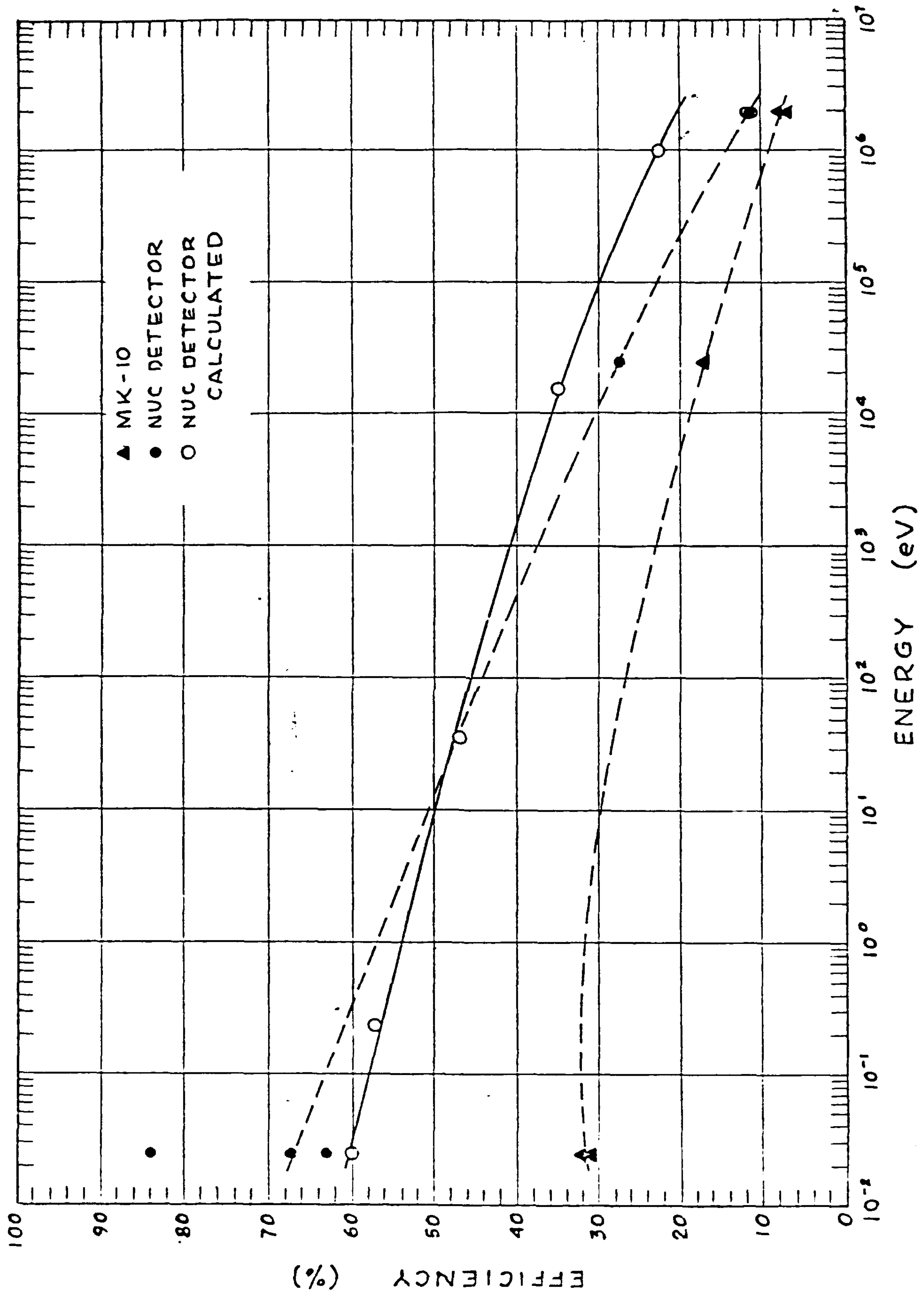

COMPARISON OF MK-10 & NUC DETECTOR EFFICIENCIES

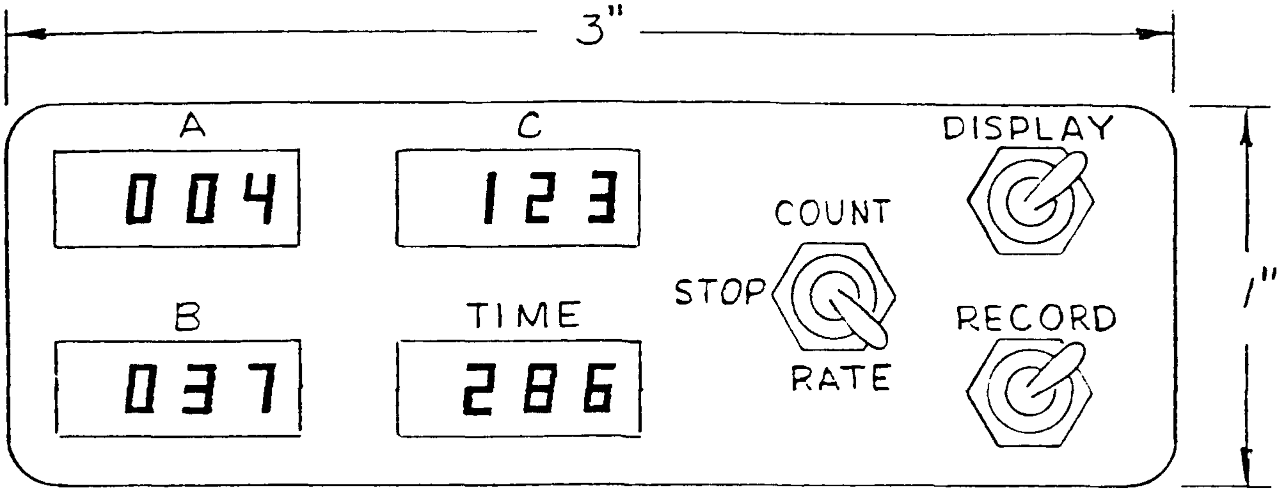

(ACCESSIBLE THROUGH PORT)

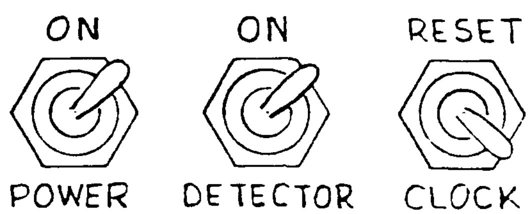

(INTERNAL)

DETECTOR CONTROL/DISPLAY ARRANGEMENT

INSTRUMENT RESPONSE TO A ^{252}CF SOURCE AT

VARIOUS DISTANCES OVER LAND AND OVER WATER

Source Strength: 2.61×10^6 n/s

Source[2] Configuration	Distance (ft)	Fraction of Counting Rate in Each Detector Section			Counting Rate[1] (c/s)
		Front	Middle	Back	
Over Land[3]	25	.34	.48	.18	150 ±1.1
	50	.37	.44	.19	40.4 ±.5
	100	.35	.44	.21	11.8 ±.2
	175	.35	.40	.25	4.4 ±.1
Over Water[4]	176	.42	.31	.27	4.4 ±.1
Background					
Over Land[3]	--	.30	.39	.30	1.72 ±.04
Over Water[4]	--	.35	.33	.32	1.67 ±.03

Notes:

1. Background subtracted.
2. Source in Pb-CH_2 Moderator.
3. Source 3 ft above asphalt pavement; detectors on pavement.
4. Source on edge of wooden pier, 4½ ft above water. Detectors 4 ft back from edge of adjacent wooden pier, 7½ ft above water. Source and detectors 160 ft from shoreline.

DRIVE-BY 45 ft FROM SOURCE AT 40 MPH

(7×10^5 n/s ^{252}Cf in Pb-CH_2 Moderator)

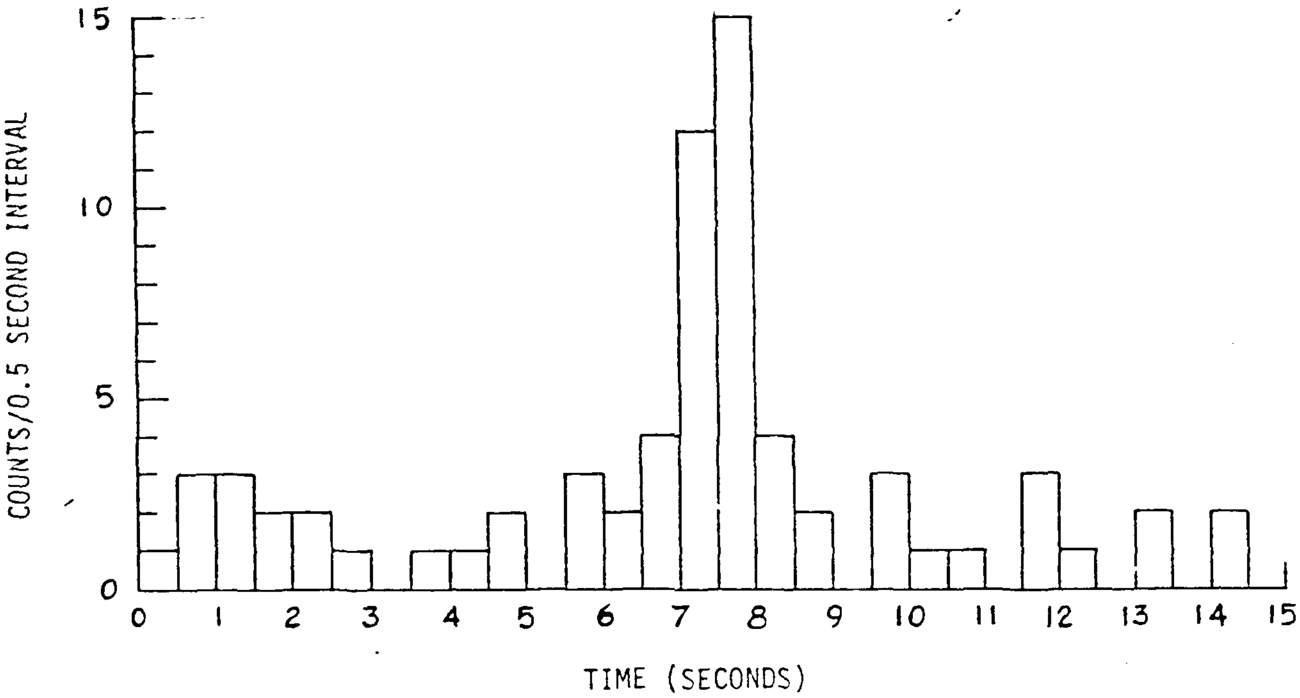

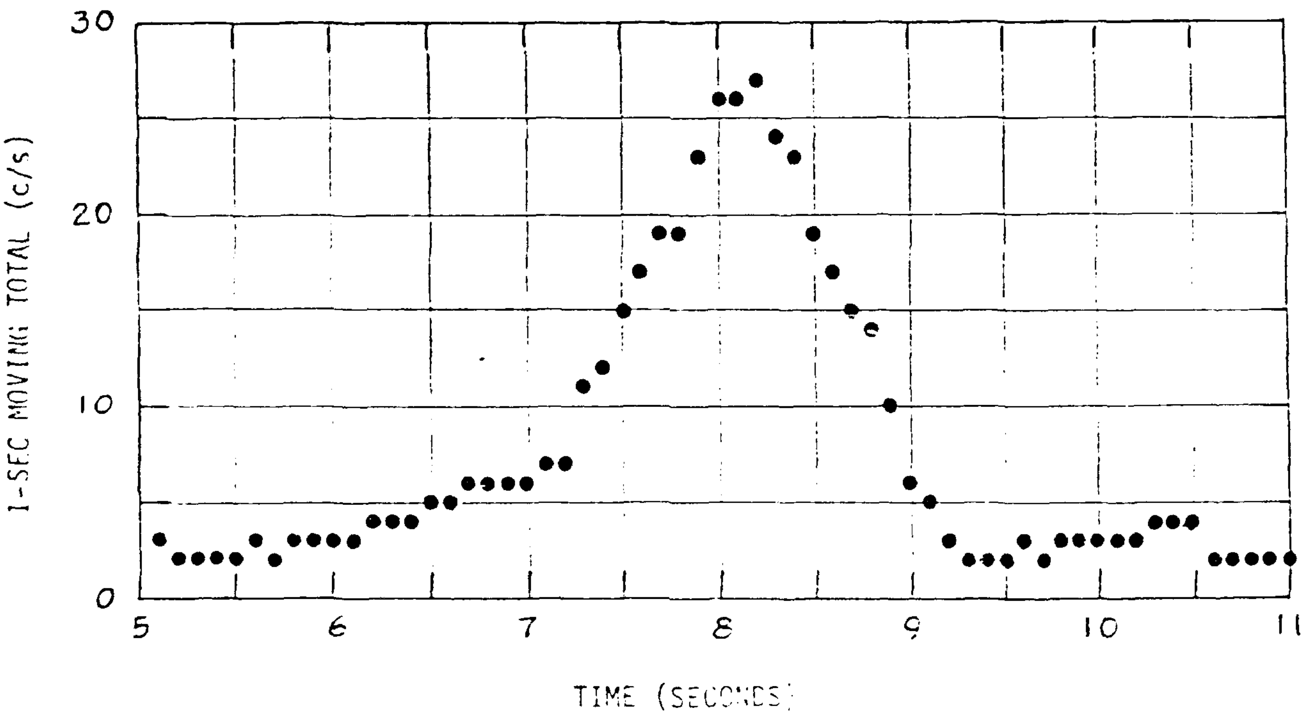

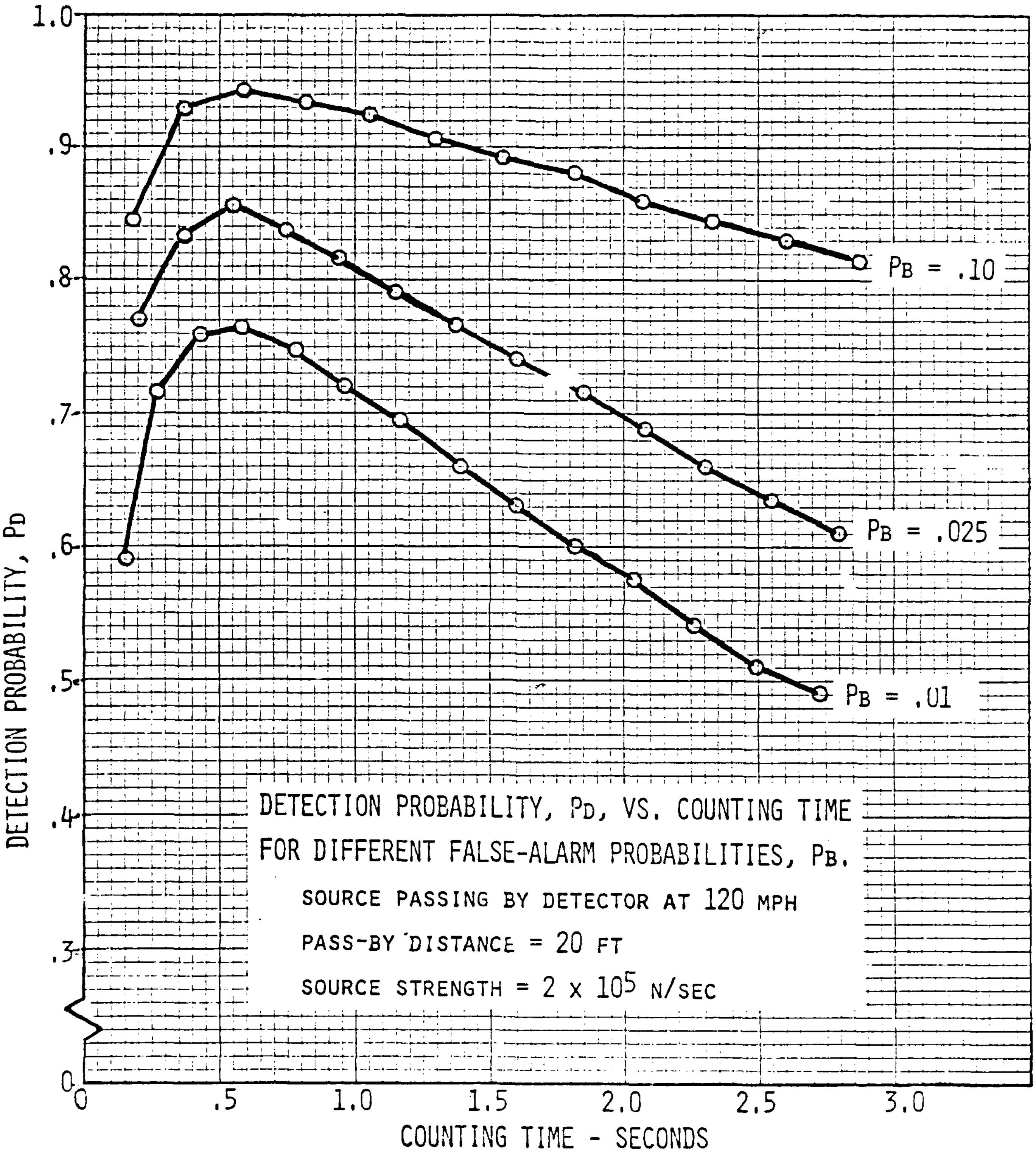
DETECTION PROBABILITY, PD
COUNTING TIME - SECONDS
1.0
.9
.8
.7
.6
.5
.4
.3
0
0
.5
1.0
1.5
2.0
2.5
3.0
PB = .10
PB = .025
PB = .01
DETECTION PROBABILITY, PD, VS. COUNTING TIME
FOR DIFFERENT FALSE-ALARM PROBABILITIES, PB.
SOURCE PASSING BY DETECTOR AT 120 MPH
PASS-BY DISTANCE = 20 FT
SOURCE STRENGTH = 2 x 10^5 N/SEC

INSTRUMENT ENERGY-DIRECTIONAL RESPONSE

Source[1] & Direction[2]		Fraction of Counting Rate in Each Detector Section			Sensitivity (cps per n/cm^2-sec)
		Front	Middle	Back	
^{252}Cf (~2Mev)	Front	.18	.66	.16	147
	Back	.17	.66	.16	146
	Top	.21	.62	.17	66
	Left	.21	.63	.17	41
	Right	.19	.62	.19	43
	Bottom	.20	.63	.17	72
^{124}Sb-Be (25Kev)	Front	.29	.60	.11	370
	Back	.18	.62	.19	362
	Top	.31	.51	.18	116
	Left	.27	.57	.16	84
	Right	.24	.57	.19	82
	Bottom	.27	.55	.18	145
Thermal[3]	Front	.82	.15	.03	875
	Back	.03	.17	.80	813
	Top	.50	.11	.39	149
	Left	.45	.18	.37	89
	Right	.41	.21	.38	108
	Bottom	.47	.08	.45	404

Notes:

1. Instrument on tower 10 ft above pavement. Source suspended approximately 5 ft above instrument.

2. Denotes side of instrument facing source.

3. ^{252}Cf source in 6-cm wall CH_2 sphere. Thermal response obtained from the difference countrate with sphere bare and with a .0075" thick Cd cover.

COMPARISON OF NUC DETECTOR AND MK-10 RESPONSES TO NEUTRON SOURCES OF DIFFERENT ENERGIES

SOURCE (1)			COUNTING RATE (c/s)			EFFICIENCY (2) (%)	
CONFIGURATION	STRENGTH (n/s)	DISTANCE (INCHES)	NUC	MK-10 (3)	RATIO	NUC	MK-10
^{124}Sb-Be	2.3×10^4	40	$63^{\pm.5}$	$41^{\pm.3}$	1.5	27	17
^{252}Cf - 10^6 BARE	2.8×10^6	72	$1000^{\pm6}$	--	--	11.2	--
MODERATED (4)	1.9×10^6	60	$2890^{\pm8}$	--	--	32	--
MOD. w/Cd (5)	1.5×10^6	60	$1570^{\pm6}$	--	--	22	--
THERMAL (6)	4.3×10^5	60	1320	--	--	67	--
^{252}Cf - 10^5 BARE	5.3×10^5	72	$195^{\pm2.4}$	$110^{\pm.7}$	1.8	11.4	6.3
MODERATED	5.2×10^5	60	$819^{\pm2.7}$	$420^{\pm9}$ (7)	1.9	34	17
MOD. w/Cd	4.1×10^5	60	$376^{\pm1.6}$	$256^{\pm5}$ (7)	1.5	20	13
THERMAL	1.2×10^5	60	$443^{\pm3.1}$	$164^{\pm10}$ (7)	2.7	84	31
^{252}Cf - 10^4 BARE	2.6×10^4	72	$8.7^{\pm.1}$	$6.5^{\pm.1}$	1.3	10.4	7.6
MODERATED	1.9×10^4	60	$26.7^{\pm.2}$	$15.6^{\pm.2}$	1.7	30	17
MOD. w/Cd	1.5×10^4	60	$14.5^{\pm.2}$	$9.2^{\pm.1}$	1.6	21	13
THERMAL	4.2×10^3	60	$12.2^{\pm.3}$	$6.4^{\pm.2}$	1.9	63	32

NOTES:

1. DETECTOR ON TOWER 10 FT. ABOVE ASPHALT PAVEMENT; SOURCE DIRECTLY ABOVE DETECTOR. CADMIUM SHEET, .020" THK, PLACED UNDER DETECTOR.
2. EFFICIENCY BASED ON FRONTAL AREA OF DETECTOR HOUSING, NUC DETECTOR = 10 7/16" x 20"; MK-10 = 12" x 18"
3. MK-10 COUNTING RATES CORRECTED FOR .25 MSEC DEADTIME
4. MODERATOR = 6" DIA. CH_2 SPHERE WITH 6 DIA. WALL THICKNESS.
5. MODERATOR COVERED WITH .0075" THK CADMIUM SHELL
6. THERMAL SOURCE = DIFFERENCE OF MODERATOR WITH & WITHOUT CADMIUM
7. COUNTING TIME UNCERTAINTY

APPENDIX B

CONSTRUCTION OF CELLS

To reduce the possibility of contamination of the electrolyte or palladium cathode, inert materials were chosen for the construction of the electrolytic cells. The basic container (figure B-1) was a Nalage FEP Teflon wide-mouth bottle, with a modified screw closure to act as a compression fitting. The cell framework was made from a solid TFE Teflon rod to insure gas-tight integrity. Electrode penetrations were made from 316 stainless steel, as were all of the tube fittings. The anode was made by winding pure platinum wire into precut groves on the outside of the framework (38 mm diameter × 55 mm high), and the wire was insulated with FEP Teflon "spaghetti" on its return length up to the stainless steel connector. The gas recombination catalyst was a commercial unit designed to handle the gas volume generated by a 3-amp discharge rate and was suspended by a platinum wire approximately 25 mm above the electrolyte. The cathode was a "fusion grade" pure palladium purchased from Johnson Matthey. The cathode measured 6.35 mm diameter × 3.85 mm to allow for a 1-amp/cm^2 current rate through the cell. The cathode was fused to its supporting platinum wire and then baked in a vacuum oven at 475°C @ 10^{-5} torr for 72 hrs. The cathode was then cooled to room temperature still under vacuum, and the oven chamber was backfilled with pure argon were the cathode remained for 48 hours before being assembled into the cell. The electrolyte was made from natural isotopic abundance lithium and 99.9% deuterium oxide, supplied by Isotec Inc., at a concentration of 0.1 molar. All preparations and cell assembly were carried out in an argon glove box to reduce the chance of hydrogen uptake by both the palladium and the deuterium oxide.

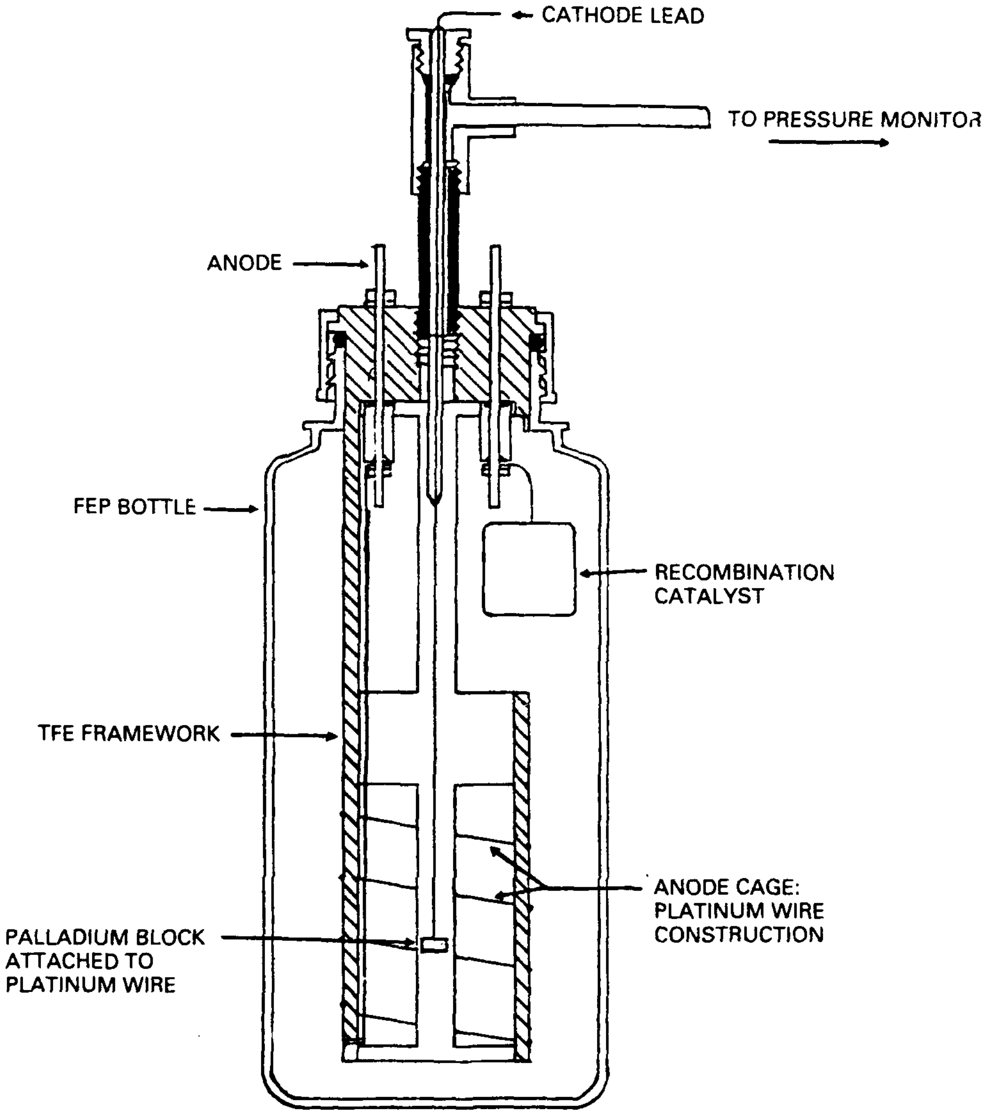

Figure B-1. CNF cell.

APPENDIX C

HELIUM MEASUREMENTS IN COLD FUSION PALLADIUM

Helium Measurements in "Cold Fusion" Palladium

B. M. Oliver
Rockwell International
Rocketdyne Division
Canoga Park CA 91303

and

K. L. Wilson
Sandia National Laboratories
Livermore CA 94551-0969

051789 A

Helium Measurements in "Cold Fusion" Palladium*

B. M. Oliver
Rockwell International
Rocketdyne Division
Canoga Park, CA 91303

and

K. L. Wilson
Sandia National Laboratories
Livermore, CA 94551

Abstract

The detection of helium products would be a most compelling piece of evidence that "cold fusion" is occurring in palladium electrochemical cells. In this paper we report on mass spectrometric measurements of helium (^3He and ^4He) released from palladium samples through vaporization. Extensive measurements conducted by Sandia National Laboratories on helium-implanted metals and metal hydrides have conclusively demonstrated that helium is not released at ambient temperatures until a He/metal concentration ratio of $\cong 0.4$ is achieved. If we assume that "cold fusion" events are creating helium in the palladium electrode with Q = 23.84 MeV, then one watt of fusion power would correspond to a helium production rate in the palladium of 2.5×10^{11} $^4He/s$.

While this potential production rate is orders of magnitude below that required for spontaneous release, it can be detected by mass spectrometry of vaporized samples. In the Rockwell International measurements, 10-50 milligram size samples were vaporized under vacuum and all gases were passed through multiple getter stages to remove unwanted gases, including hydrogen isotopes. The helium concentrations were then measured using a precision mass spectrometer. Absolute calibration of the system was verified using palladium samples implanted with 700 keV ^4He ions. The ultimate detection level of the system is $\approx 1 \times 10^{10}$ helium atoms (either ^3He or ^4He or both) per gram of palladium. Results of helium measurements conducted for a number of U.S. laboratories are presented. In no case was there any "cold fusion" helium detected above system background for palladium electrodes used typically for 1-2 weeks, implying a maximum time-averaged "cold fusion" rate of less than 0.1 microwatts.

* This work supported by the U.S. Dept. of Energy

Acknowledgements

Rockwell International

H. Farrar
D. W. Kneff
G. Subbaramman
J. R. Szekeres

Sandia National Laboratories Livermore

M. I. Baskes
T. E. Felter
S. E. Guthrie
B. V. Hess
M. E. Malinowski
G. J. Thomas

This work was supported by the U.S. DOE

051789B

OUTLINE

I. Introduction

II. Review of the Behavior of Helium in Palladium and Palladium Tritide

III. Experimental Procedure

IV. "Cold Fusion" Results

V. Conclusion

051789 C

I. Introduction

All of the Popular "Cold Fusion" Reactions Produce Helium

$$d + d \longrightarrow T + p + 4\ \text{MeV}$$
$$T \longrightarrow {}^{3}\text{He} + \beta^{-} + \overline{\nu}_e$$

$$d + d \longrightarrow {}^{4}\text{He} + 23.85\ \text{MeV}$$

$$d + {}^{6}\text{Li} \longrightarrow {}^{4}\text{He} + {}^{4}\text{He} + 22.37\ \text{MeV}$$

$$d + d \longrightarrow {}^{3}\text{He} + n + 3.3\ \text{MeV}$$

051789 E

II. Review of the Behavior of Helium in Palladium and Palladium Tritide

051789 F

Helium is Strongly Trapped in Palladium and Palladium Hydride

Extensive studies have been conducted on ^{4}He implanted into metals and metal hydrides and on ^{3}He release from metal tritides.

- Helium has a high diffusivity but is strongly trapped at defects due to low solubility

- Helium self-clustering produces its own defects by creation of a self-interstitials and eventually $\simeq$ 2 nm bubbles

- Helium is retained in palladium until annealing temperatures in excess of 600 °C are achieved for dilute concentrations

- Spontaneous helium release at room temperature is not observed until the helium/metal ratio exceeds 0.1

051789 G

Helium is Retained in Metal Tritides Until Its Concentration Exceeds 0.1 Helium/Metal Ratio

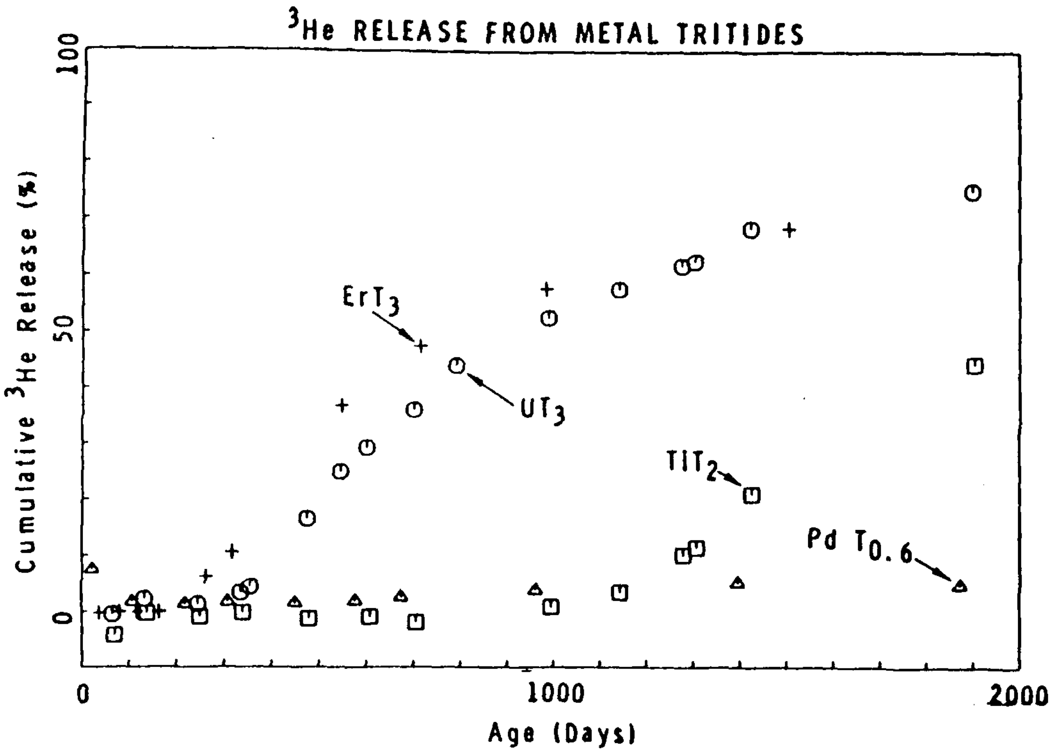

M. E. Malinowski (1976)

Onset of Spontaneous (Accelerated) Release	
UT_3, ErT_3	0.15 He/M
Ti T_2	0.3 He/M
Pd $T_{0.6}$	0.4 He/M

051889 A

Implanted Helium is Retained in Palladium Until the Helium/Metal Ratio Reaches 0.4

HELIUM SATURATION BEHAVIOR
RE-EMISSION MEASUREMENTS IN PALLADIUM

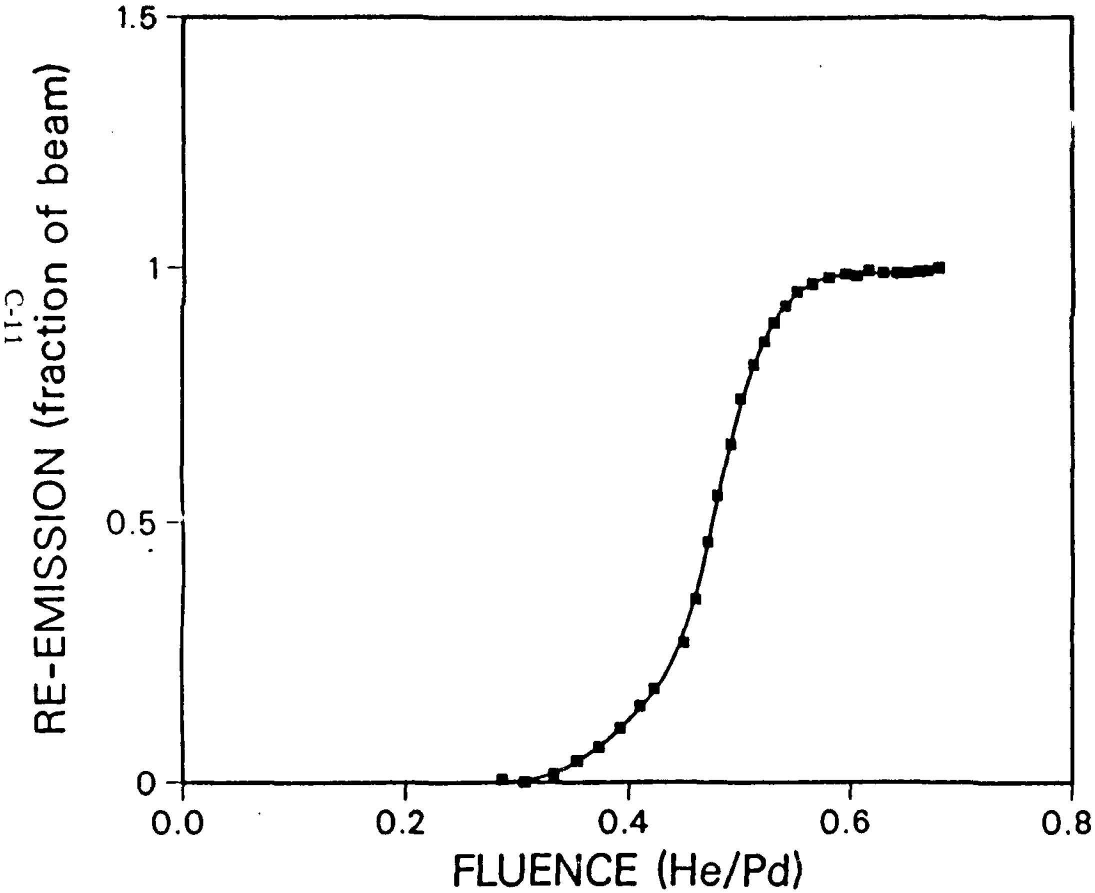

- Room Temperature Implantation
- 1 keV $^{4}He^{+}$
- 10^{14} $He/cm^2 \cdot s$

051889 B

Helium is Retained in Palladium to Elevated Temperatures

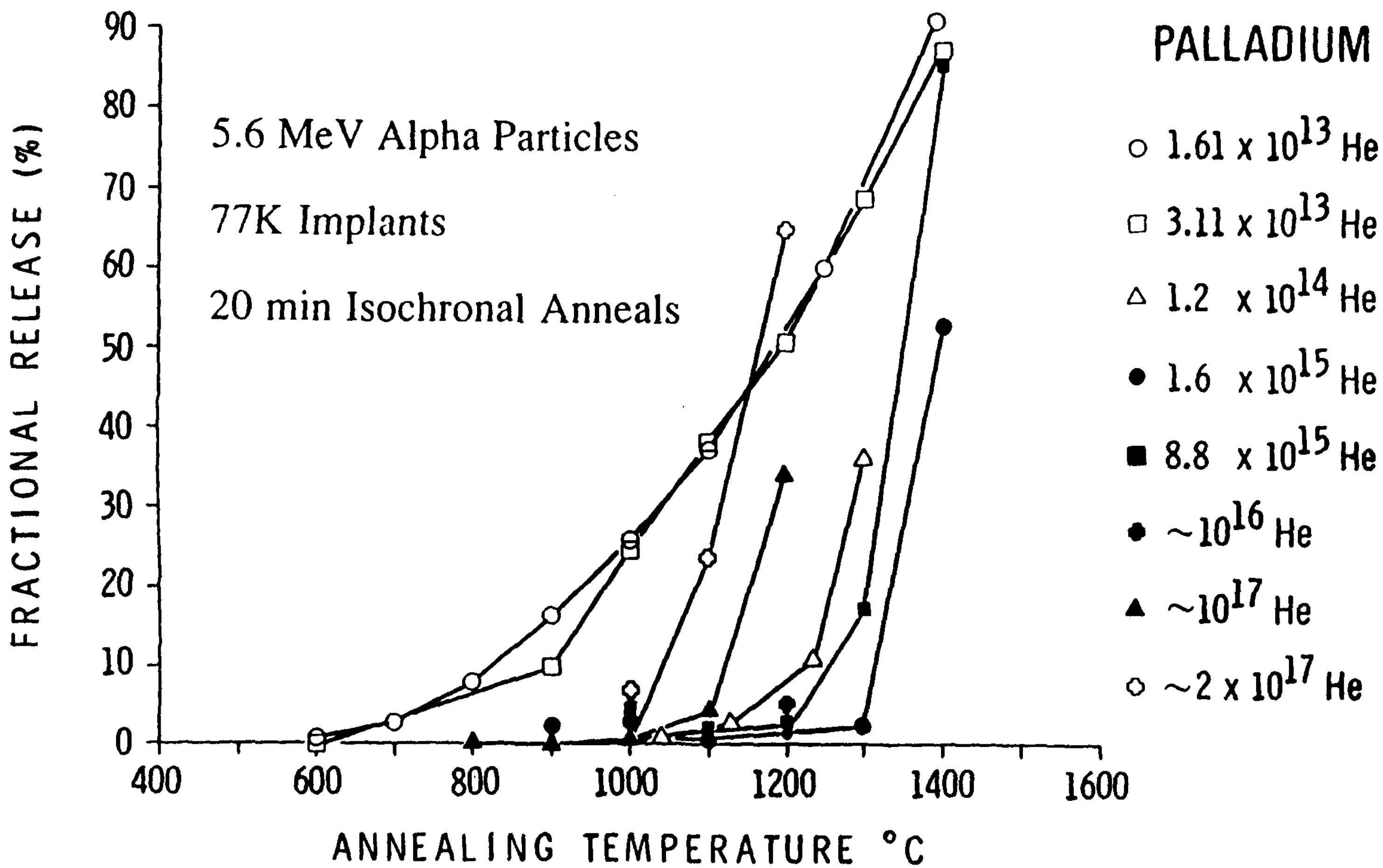

Our computations show that helium atoms force metal atoms from their natural position to create bubbles

Initial conditions Equilibrium position

Molecular Dynamics Calculations Using the Embedded Atom Method Predict He Bubble Formation in $PdT_{0.6}$

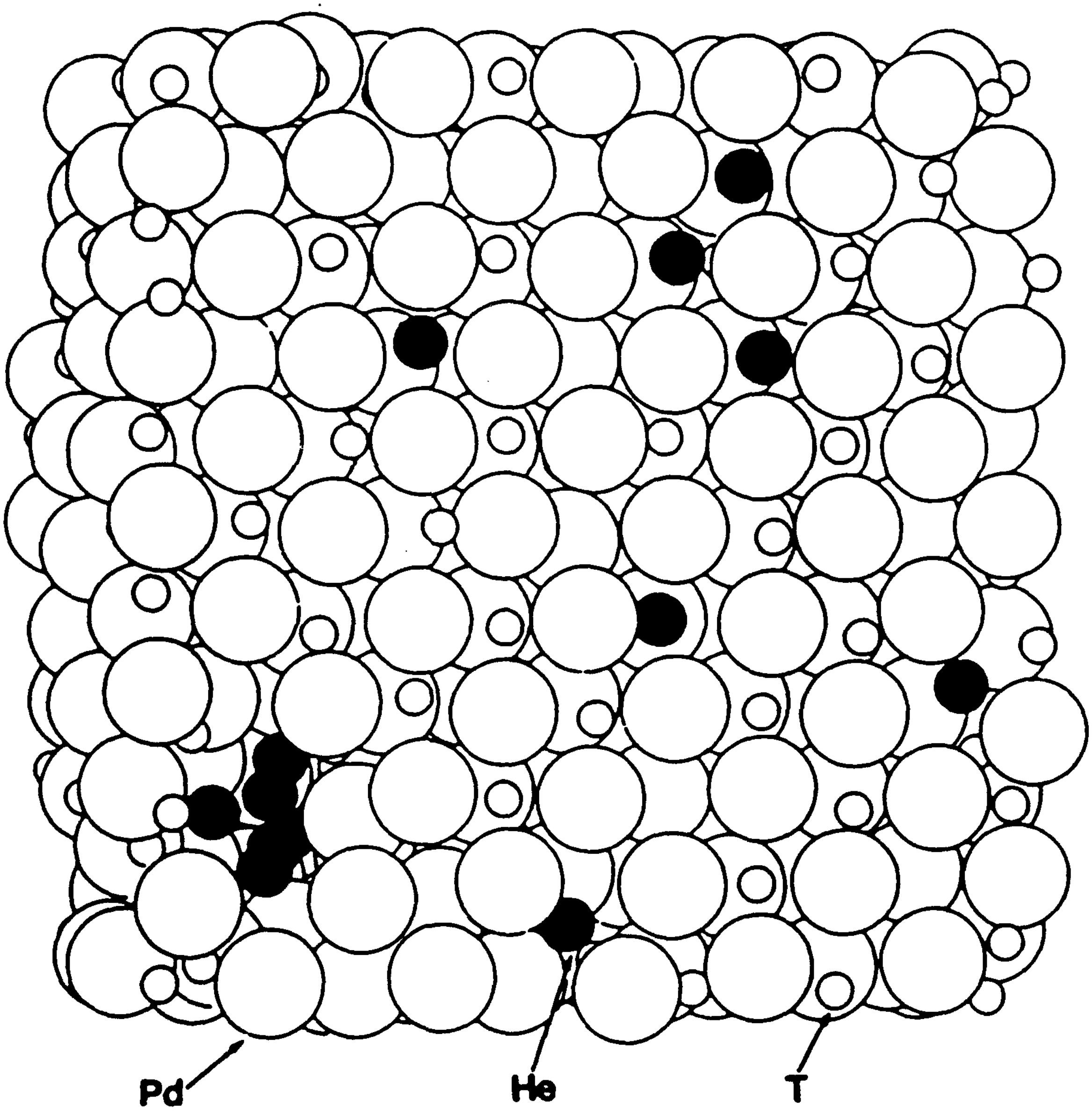

051889 D

Helium Bubbles in Palladium Tritide (1 at. % Helium)

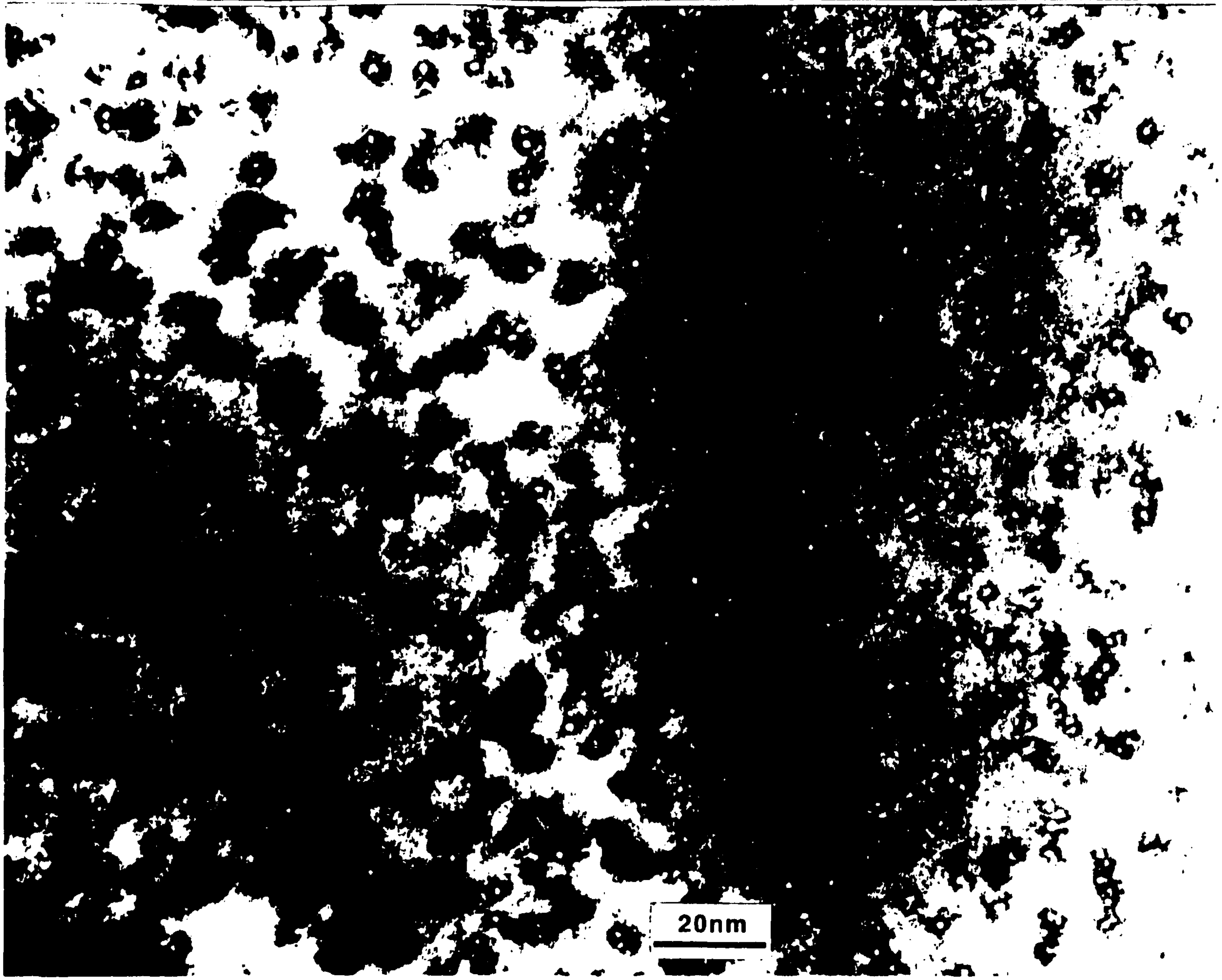

III. Experimental Procedure

HELIUM MASS SPECTROMETER SYSTEM

THE HELIUM MASS SPECTROMETER SYSTEM AT ROCKETDYNE IS A UNIQUE U.S. GOVERNMENT OWNED CENTRALIZED FACILITY DEDICATED TO LOW-LEVEL HELIUM MEASUREMENTS IN SOLIDS AND SELECTED LIQUIDS

- PERMANENT MAGNET INSTRUMENT (2 IN. RADIUS, 60 DEGREE DEFLECTION, $\Delta M/M \sim 1/100$) OPERATING IN STATIC MODE
- MULTIPLE GETTERS TO REMOVE HYDROGEN ISOTOPES AND ACTIVE GASES
- ON-LINE MULTIPLE HELIUM "SPIKING" SYSTEMS FOR ISOTOPE-DILUTION ANALYSIS
- DYNAMIC RANGE FROM PERCENT LEVELS TO 10^{-12} ATOM FRACTION (PARTS-PER-TRILLION)
- CAN ANALYZE SOLID SAMPLES FROM MICROGRAMS TO GRAMS
- 1% ABSOLUTE ACCURACY OVER MOST OF MEASUREMENT RANGE
- CAN ACCURATELY AND INDEPENDENTLY DETERMINE TRITIUM IN SOLIDS OR LIQUIDS BY MEASUREMENT OF DECAY PRODUCT, ^{3}He
  - INDEPENDENT METHOD FROM NUCLEAR MEASUREMENTS

MASS SPECTROMETER SYSTEM

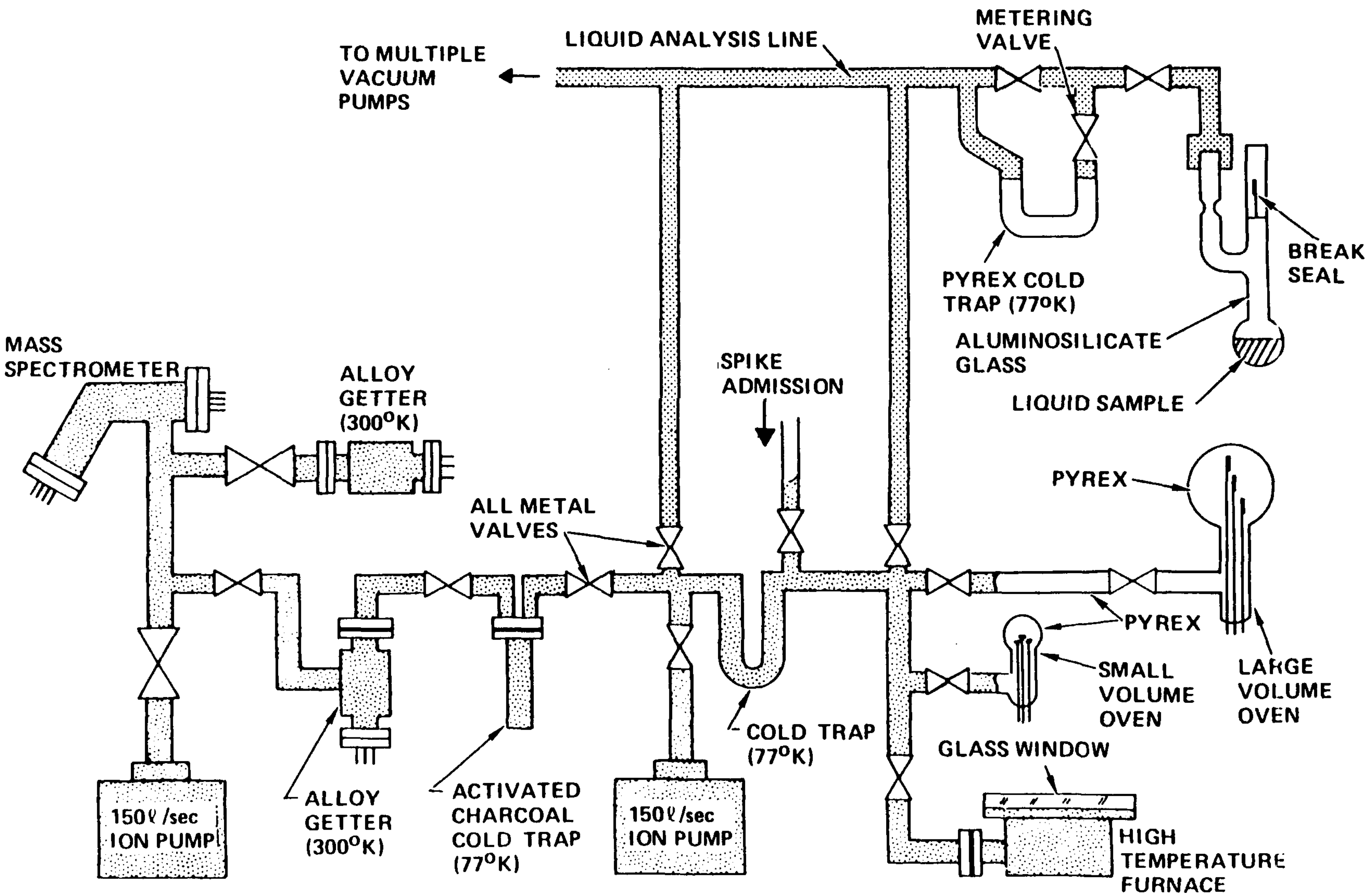

SECTION OF HELIUM "SPIKE" SYSTEM

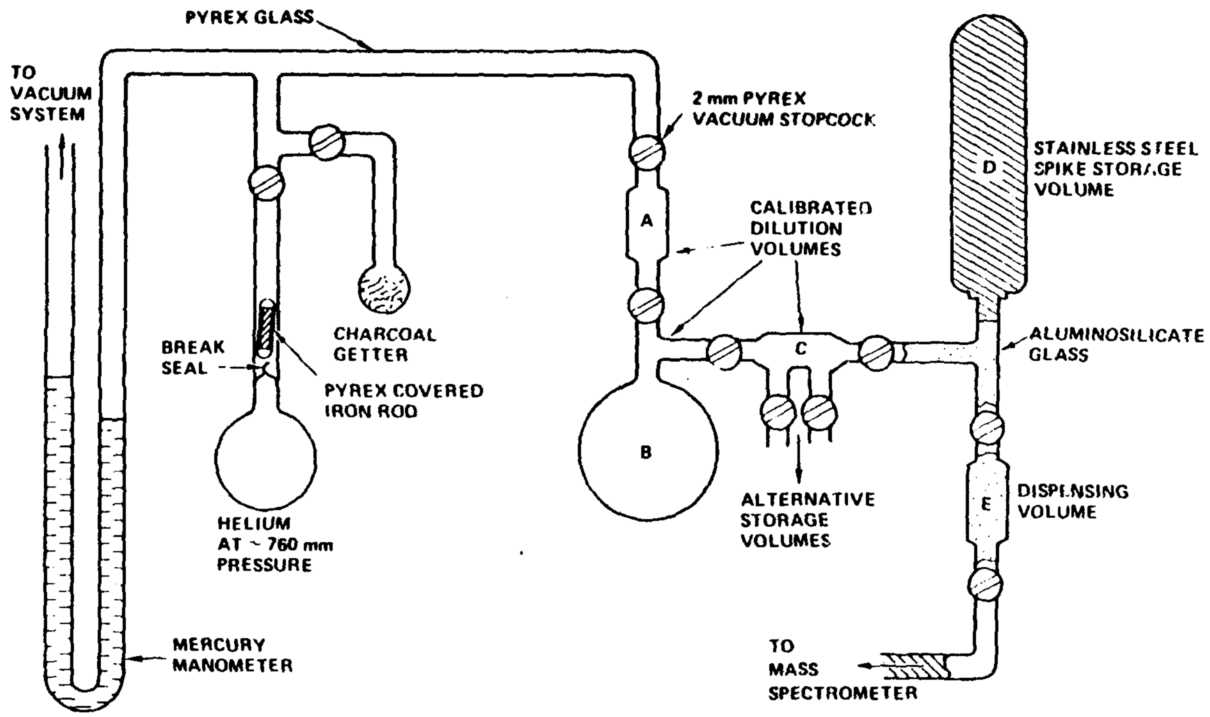

ANALYSIS LINE FOR TRITIUM SOLUTIONS

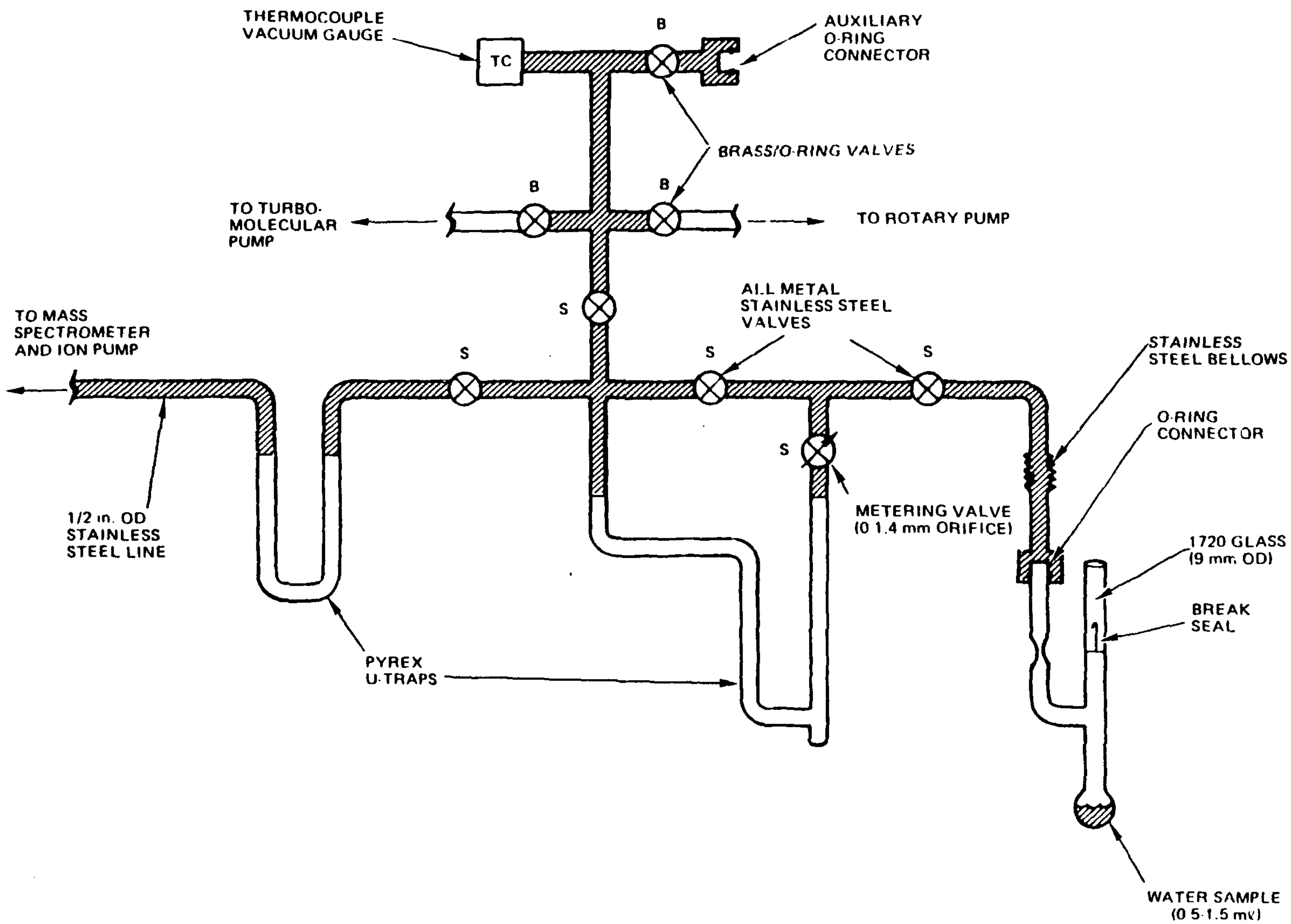

RESULTS OF HELIUM ANALYSES ON ION-IMPLANTED PALLADIUM

SAMPLE	DESCRIPTION	FURNACE	^{4}He CONTENT (10^{11} ATOMS) MEASURED	CALCULATED
Pd-1	8 mm dia.	Graphite[1]	1.06 (.03)	1.000
-2	Pd Disk	Graphite	1.03 (.03)	0.999
-3		CTF[2]	1.04 (.02)	1.000
-4		CTF	1.03 (.02)	0.998
Pd-7	8 mm dia.	CTF	0.116 (.008)	0.100
-8	Pd Disk	CTF	0.111 (.008)	0.100
-9		CTF	0.108 (.008)	0.101
-10		Coil[3]	0.097 (.005)	0.102
-11		Coil	0.108 (.005)	0.100

(1) GRAPHITE CRUCIBLE (~3700 DEG. C)
(2) GRAPHITE CONSTANT-TEMPERATURE FURNACE (~2000 DEG. C)
(3) TUNGSTEN-WIRE COIL (~3400 DEG. C)

CALIBRATION VERIFICATION OF MASS SPECTROMETER SYSTEM

ABSOLUTE ACCURACY OF THE HELIUM ANALYSIS SYSTEM VERIFIED OVER 20 YEARS

- HELIUM IN EARTHS' ATMOSPHERE (GEO. COSM. ACTA 48, 1759 (1983))
- CORRECTION OF NIST (NBS) TRITIUM STANDARD (INT. J. APPL. RAD. ISOT. A40, 199 (1989))
- MEASUREMENT OF TRITIUM HALF-LIFE (INT. J. APPL. RAD. ISOT. A38, 959 (1987))

ACCURACY FOR PALLADIUM WAS CHECKED BY ANALYSES OF ION-IMPLANTED SAMPLES.

- MATERIAL: PALLADIUM FOIL, 0.1 MM X 8 MM O.D.
- SIX FOILS EACH WERE IMPLANTED TO CALCULATED DOSES OF 10^{10} AND 10^{11} ATOMS OF ^{4}HE (AT SNLL)
- COMPLETE FOILS WERE ANALYZED FOR ^{4}HE IN THE SAME FURNACES USED FOR "COLD FUSION" ANALYSES
- RESULTS WERE IN AGREEMENT (WITHIN UNCERTAINTIES) WITH CALCULATED IMPLANTED AMOUNTS

HELIUM ANALYSIS PROCEDURE FOR PALLADIUM

DUPLICATE HELIUM ANALYSES ARE CONDUCTED ON EACH RECEIVED SAMPLE

- EACH SAMPLE WAS EXAMINED UNDER LOW-POWER STEREO MICROSCOPE TO CHECK FOR INTEGRITY
- TWO 10 TO 20 MG SAMPLES WERE CUT FROM ADJACENT REPRESENTATIVE LOCATIONS ON EACH SAMPLE
- EACH SPECIMEN WAS LOADED INTO A TUNGSTEN-WIRE CRUCIBLE IN HIGH-SENSITIVITY VACUUM OVEN
- EACH SPECIMEN WAS VAPORIZED, AND ALL RELEASED GASES PASSED THROUGH GETTERS INTO MASS SPECTROMETER
- MEASURED $^{3}He/^{4}He$ WAS COMPARED TO KNOWN ALIQUOTS OF HELIUM "SPIKES"
- MASS DISCRIMINATION OF SYSTEM WAS MEASURED EACH DAY BY ANALYSIS OF KNOWN COMBINATIONS OF ^{3}He AND ^{4}He SPIKES

IV. "Cold Fusion" Results

051889 H

HELIUM ANALYSIS RESULTS ON "COLD FUSION" PALLADIUM

LABORATORY	SAMPLE	DESCRIPTION	SAMPLE MASS (MG)	MEASURED HELIUM (10^9 ATOMS) ^{3}He (1σ)	^{4}He (1σ)
LLNL	Pd1-A (Control)	1 mm dia.	16.97	<0.1 (0.8)	<0.1 (0.3)
	Pd1-B (Control)	helical coil	16.10	<0.1 (0.8)	<0.1 (0.3)
LLNL	Pd2-A (D_2O)	1 mm dia.	14.93	0.7 (0.8)	0.3 (0.3)
	Pd2-B (D_2O)	helical coil	17.81	0.6 (0.8)	<0.1 (0.3)
SNLL	Pd1-A (Control)	3 mm dia.	9.71	6.3* (0.8)	<0.1 (0.3)
	Pd1-B (Control)	Pd rod	16.21	0.8 (0.8)	9.0* (0.3)
SNLL	Pd2-A (D_2O)	3 mm dia.	17.98	<0.1 (0.8)	2.3* (0.3)
	Pd2-B (D_2O)	Pd rod	17.23	1.2 (0.8)	0.3 (0.3)
MIT	Pd1-A (Control)	1 mm dia.	13.60	<0.1 (0.8)	0.2 (0.4)
	Pd1-B (Control)	Pd wire	18.52	<0.1 (0.8)	<0.1 (0.4)
MIT	Pd2-A (D_2O)	1 mm dia.	12.29	<0.1 (0.8)	<0.1 (0.4)
	Pd2-B (D_2O)	Pd wire	12.64	<0.1 (0.8)	0.4 (0.4)

NOSC	PD1-A (CONTROL) PD1-B (CONTROL)	2 ~~4~~ MM DIA. PD ROD	19.54 19.07	<0.1 (1.5) 1.9 (0.8)	3.7*(0.6) <0.1 (0.5)
NOSC	PD2-A (D_2O) PD2-B (D_2O)	~4 ~~2~~ MM DIA. PD WIRE	11.86 15.29	<0.1 (1.5) <0.1 (0.8)	<0.1 (0.6) 0.3 (0.5)
NOSC	PD3-A (D_2O) PD3-B (D_2O)	~4 MM DIA. PD ROD	17.84 13.07	4.0*(0.8) 1.5 (1.5)	0.4 (0.5) <0.1 (0.6)
ETT	PD1-A (CONTROL) PD1-B (CONTROL)	1 MM DIA. PD WIRE	16.01 17.75	<0.1 (0.8) <0.1 (0.8)	<0.1 (0.2) <0.1 (0.4)
ETT	PD2-A (CONTROL) PD2-B (CONTROL)	1 MM DIA. PD WIRE	10.33 11.22	<0.1 (0.8) 0.3 (0.8)	<0.1 (0.2) <0.1 (0.4)
ETT	PD3-A (D_2O) PD3-B (D_2O)	1 MM DIA. PD WIRE	13.83 14.22	0.9 (0.8) 0.3 (0.8)	0.3 (0.2) <0.1 (0.4)
ETT	PD4-A (D_2O) PD4-B (D_2O)	1 MM DIA. PD WIRE	13.39 13.31	<0.1 (0.8) 0.7 (0.8)	<0.1 (0.2) <0.1 (0.4)
ETT	PD5-A (D_2O) PD5-B (D_2O)	1 MM DIA. PD WIRE	14.88 9.85	0.2 (1.0) 1.3 (1.0)	<0.1 (0.2) <0.1 (0.2)
ORNL	PD1-A (CONTROL) PD1-B (CONTROL)	6.4 MM PD SHEET	10.76 13.38	<0.1 (0.9) <0.1 (4.0)	<0.1 (0.6) 0.8 (0.5)
ORNL	PD2-A (D_2O) PD2-B (D_2O)	6.4 MM PD SHEET	10.35 12.79	1.3 (0.9) 0.3 (4.0)	0.2 (0.6) 0.4 (0.5)

ORNL	Ti1-A (Control)	0.64 mm Ti	1.635	0.6 (0.9)	<0.1 (0.6)
	Ti1-B (Control)	sheet	5.442	3.5 (4.0)	0.7 (0.5)
ORNL	Ti2-A (D_2O)	0.64 mm Ti	2.634	18.0*(0.9)	<0.1 (0.6)
	Ti2-B (D_2O)	sheet	6.297	1.7 (4.0)	0.1 (0.5)
A&M	Pd1-A (Control)	1 mm dia.	14.19	<0.1 (1.2)	0.1 (0.3)
	Pd1-B (Control	Pd wire	14.49	0.2 (0.8)	<0.1 (0.2)
A&M	Pd2-A (D_2O)	1 mm dia.	11.72	<0.1 (1.2)	<0.1 (0.3)
	Pd2-B (D_2O)	Pd wire	13.56	0.2 (0.8)	<0.1 (0.2)
A&M	Pd3-A (Control)	1 mm dia.	9.14	<0.1 (1.2)	0.1 (0.3)
	Pd3-B (Control	Pd wire	10.74	<0.1 (0.8)	<0.1 (0.2)
A&M	Pd4-A (D_2O)	2 mm dia.	9.18	<0.1 (1.2)	<0.1 (0.3)
	Pd4-B (D_2O)	Pd sphere	8.79	<0.1 (0.8)	<0.1 (0.2)

*Values were not reproduced on the duplicate specimen, and, in the absence of verification, are assumed to be from an anomalously high background

LLNL = LAWRENCE LIVERMORE NATIONAL LABORATORY
SNLL = SANDIA NATIONAL LABORATORIES - LIVERMORE
MIT = MASSACHUSETTS INSTITUTE OF TECHNOLOGY
NOSC = NAVAL OCEAN SYSTEM CENTER, SAN DIEGO, CALIFORNIA.
ETT = ELECTRON TRANSFER TECHNOLOGIES, INC.
ORNL = OAK RIDGE NATIONAL LABORATORY
A&M = TEXAS A&M UNIVERSITY

V. Conclusions

051889 I

CONCLUSIONS

- ABSOLUTE ACCURACY OF MASS SPECTROMETER SYSTEM VERIFIED BY MANY PUBLISHED COMPARISONS OVER 20 YEARS

- DETECTION LIMITS FOR MASS SPECTROMETER SYSTEM:

  - $\sim 8 \times 10^8$ ATOMS ^3He (1σ)
  - $\sim 2 \times 10^8$ ATOMS ^4He (1σ)

- ANALYSES OF "COLD FUSION" ELECTRODE MATERIAL FROM 8 DIFFERENT LABORATORIES AND 14 EXPERIMENTS, SHOWED:

  - <u>NO</u> SIGNIFICANT DIFFERENCE BETWEEN ELECTROLYZED MATERIAL AND "AS-RECEIVED" MATERIAL
  - <u>NO</u> SIGNIFICANT ^3He OR ^4He ABOVE ANALYSIS LIMITS
  - OCCASIONAL OBSERVED $^3He/^4He$ ABOVE ANALYSIS LIMITS ARE NOT CONFIRMED

- HELIUM RESULTS ON COLD FUSION ELECTRODES INDICATE <u>UPPER LIMITS</u> FOR COLD FUSION POWER OUTPUT TO BE:

  - MICROWATTS/CC FOR D + D -> ^4He
  - MICROWATTS/CC FOR D + D -> n + ^3He
  - MILLIWATTS/CC FOR D + D -> p + ^3H (DECAY TO ^3He)

REPORT DOCUMENTATION PAGE

Form Approved OMB No. 0704-0188

1. AGENCY USE ONLY *(Leave blank)*	2. REPORT DATE	3. REPORT TYPE AND DATES COVERED
	March 1991	Final: 1989

4. TITLE AND SUBTITLE	5. FUNDING NUMBERS
COLD FUSION VERIFICATION	DN300012 0601152N ZW25 RR000N0
6. AUTHOR(S) M. H. North, G. F. Mastny, and E. J. Wesley	
7. PERFORMING ORGANIZATION NAME(S) AND ADDRESS(ES) Naval Ocean Systems Center San Diego, CA 92152–5000	8. PERFORMING ORGANIZATION REPORT NUMBER NOSC TR 1412
9. SPONSORING/MONITORING AGENCY NAME(S) AND ADDRESS(ES) Office of Chief of Naval Research Independent Research Program Arlington, VA 22217–5000	10. SPONSORING/MONITORING AGENCY REPORT NUMBER OCNR-10P

11. SUPPLEMENTARY NOTES

12a. DISTRIBUTION/AVAILABILITY STATEMENT	12b. DISTRIBUTION CODE
Approved for public release; distribution is unlimited.	

13. ABSTRACT *(Maximum 200 words)*

This report attempts to verify and reproduce experimental observations of Cold Nuclear Fusion (CNF), as originally reported in 1989. The conclusion is that CNF probably is chimera and will go the way of N-rays and polywater.

14. SUBJECT TERMS	15. NUMBER OF PAGES
fractofusion cold nuclear fusion	63
	16. PRICE CODE

17. SECURITY CLASSIFICATION OF REPORT	18. SECURITY CLASSIFICATION OF THIS PAGE	19. SECURITY CLASSIFICATION OF ABSTRACT	20. LIMITATION OF ABSTRACT
UNCLASSIFIED	UNCLASSIFIED	UNCLASSIFIED	SAME AS REPORT

INITIAL DISTRIBUTION

Code 0012	Patent Counsel	(1)
Code 014	W. T. Rasmussen	(1)
Code 0141	A. Gordon	(1)
Code 0144	R. November	(1)
Code 50	H. O. Porter	(1)
Code 52	Acting Head	(1)
Code 524	Acting Head	(1)
Code 524	M. North	(10)
Code 60	F. E. Gordon	(1)
Code 63	R. H. Moore	(1)
Code 634	L. A. Parnell	(1)
Code 952B	J. Puleo	(1)
Code 961	Archive/Stock	(6)
Code 964B	Library	(3)

Defense Technical Information Center
Alexandria, VA 22304-6145 (4)

NOSC Liaison Office
Washington, DC 20363-5100

Center for Naval Analyses
Alexandria, VA 22302-0268

Navy Acquisition, Research & Development
Information Center (NARDIC)
Alexandria, VA 22333

Michigan Technological University
Houghton, MI 49931

Los Alamos National Laboratory
Los Alamos, NM 87545